AMERICAN MUSEUM NOVITATES

Number 4000, 36 pp. June 28, 2023

Systematic Revision of the Whip Spider Family Paracharontidae (Arachnida: Amblypygi) with Description of a New Troglobitic Genus and Species from Colombia

JAIRO A. MORENO-GONZÁLEZ,[1] MIGUEL GUTIERREZ-ESTRADA,[2] AND LORENZO PRENDINI[1]

ABSTRACT

The ancient, enigmatic whip spider family Paracharontidae Weygoldt, 1996, representing the basalmost lineage of the arachnid order Amblypygi Thorell, 1883, is revised. The monotypic West African genus *Paracharon* Hansen, 1921, from Guinea Bissau, is redescribed, based on a reexamination and reinterpretation of the newly designated lectotype. A new troglobitic whip spider, *Jorottui ipuanai*, gen. et sp. nov., is described from a cave system in the upper basin of the Camarones River in the La Guajira Department of northeastern Colombia. This new taxon is the second extant representative of Paracharontidae and the first outside Africa. It is unambiguously assigned to the family based on several characters shared with *Paracharon caecus* Hansen, 1921, notably a projection of the anterior carapace margin, the tritosternum not projecting anteriorly, similar pedipalp spination, a reduced number of trichobothria on the tibia of leg IV, and cushionlike female gonopods. A detailed examination confirmed the absence of ocelli in both genera and the presence of three (*Paracharon*) vs. four (*Jorottui*, gen. nov.) prolateral teeth on the basal segment of the chelicera, the dorsalmost tooth bicuspid in both genera. The male gonopods of Paracharontidae are described for the first time. *Paracharonopsis cambayensis* Engel and Grimaldi, 2014, is removed from Paracharontidae and placed incertae sedis in Euamblypygi Weygoldt, 1996; amended, comparative diagnoses are presented for

[1] Arachnology Lab, Division of Invertebrate Zoology, American Museum of Natural History.

[2] Programa de Posgrado "Gestión Integral Frente al Cambio Climático," Grupo de Investigación Territorios Semiáridos del Caribe, Facultad de Ingeniería, Universidad de la Guajira, Riohacha, Colombia.

 ISSN 0003-0082

Paracharontidae and *Paracharon*; and previous interpretations of various diagnostic characters for Paracharontidae are discussed.

INTRODUCTION

The order Amblypygi Thorell, 1883, popularly known as whip spiders or tailless whip scorpions, is a small order of arachnids with dorsoventrally flattened bodies, conspicuous raptorial pedipalps, and the first pair of legs antenniform (Weygoldt, 2000a, 2002; Prendini et al., 2005). Amblypygi is the sister group of Uropygi Thorell, 1883, the group that comprises the whip scorpion orders Schizomida Petrunkevitch, 1945, and Thelyphonida Latreille, 1804. Together, the three orders constitute Pedipalpi Borner, 1904, a clade consistently supported by genotypic and phenotypic evidence (Shultz, 1990, 2007; Legg et al., 2013; Garwood and Dunlop, 2014; Giribet, 2018; Ballesteros et al., 2022).

Amblypygi currently includes two suborders, five recent families, 17 genera, and 262 species, as well as eight fossil genera and 13 fossil species, primarily distributed in subtropical and tropical habitats (WAC, 2023). The diversity contained within each of the two suborders of Amblypygi is highly asymmetric, however. Suborder Euamblypygi Weygoldt, 1996, distributed on all continents except Antarctica, comprises four families and the vast majority of whip spider genera and species (Weygoldt, 2000a; WAC, 2023) whereas suborder Paleoamblypygi Weygoldt, 1996, is represented by a single taxon, *Paracharon caecus* Hansen, 1921, placed in Paracharontidae Weygoldt, 1996, and restricted to West Africa.

Hansen (1921) described *P. caecus* from 17 morphologically unique adult specimens, 16 of which were collected inside termitaria, during an expedition by Leonardo Fea to Bolama and Rio Cassine in Guinea Bissau. Hansen (1921) considered the species closely related to the family Charontidae Simon, 1892, but placed it in a monotypic genus due to the absence of ocelli and the structure of the sternal labium (tritosternum). Decades later, Quintero (1986) placed *Paracharon* Hansen, 1921, in the family Charinidae Quintero, 1986, within Pulvillata, based on a manual cladistic analysis of nine terminals and 17 morphological characters. Quintero (1986) noted that the conspicuous projection of the anterior carapace margin of *Paracharon*, first described by Hansen (1921), resembled fossils such as *Graeophonus anglicus* Scudder, 1879 (= *Weygoldtina anglica* Pocock, 1911), as first pointed out by Petrunkevitch (1955).

Weygoldt (1996) subsequently presented the second phylogenetic reconstruction of Amblypygi based on an analysis of 18 genera and 29 morphological characters, conducted with the phylogenetic-analysis software Hennig86. Weygoldt (1996) provided additional observations about the morphology of *P. caecus*, including the vertical orientation of the pedipalps; only two dorsal spines on the pedipalp femur; a reduced number of spines on the pedipalp tibia (patella); four prolateral teeth (dorsalmost tooth simple) on the basal segment of the chelicera; and the absence of ventral sacs. As previous authors, Weygoldt (1996) noted the similarity of the carapace shape, especially the projection of its anterior margin, to fossils such as *Graeophonus anglicus*. Weygoldt's (1996) analysis placed *Paracharon* as the sister group of all other extant whip spiders due to the presence of numerous plesiomorphic character states. This led Weygoldt (1996) to propose a new classification, accommodating *Paracharon* within the monotypic family Paracharontidae and the suborder Paleoamblypygi.

Following Weygoldt's (1996) analysis, several authors referred to *P. caecus* as a "living-fossil" (e.g., Weygoldt, 2000a, 2000b, 2002; Dunlop et al., 2008; Engel and Grimaldi, 2014) and a second species of Paracharontidae, *Paracharonopsis cambayensis* Engel and Grimaldi, 2014, was described from Early Eocene amber in the Cambay Basin of Gujarat, India. More recently, Garwood et al. (2017) reexamined the morphology of one of the syntypes of *P. caecus* in the context of a phylogenetic analysis of extinct Amblypygi. Garwood et al. (2017) claimed that *Paracharon* possesses lateral ocelli and shares with *G. anglicus* the presence of vertically oriented pedipalps and a simple distalmost prolateral tooth on the basal segment of the chelicera. The analysis of Garwood et al. (2017) recovered Paleoamblypygi, composed of Paracharontidae (the group comprising *Paracharon* and *Paracharonopsis* Engel and Grimaldi, 2014) and *Graeophonus*, and supported by two synapomorphies: carapace margin with anterior projection; pedipalps vertically oriented. Paracharontidae was supported by two synapomorphies: dorsal spines present on the pedipalp tarsus; three dorsal spines and three ventral spines on the pedipalp patella.

Despite these advances, some of the most widely accepted diagnostic characters of Paracharontidae, such as the projection of the anterior carapace margin, were challenged, as was the placement of *P. cambayensis* in the family (Haug and Haug, 2021). Until recently, no new paracharontid material had been collected since the original description over a century ago. Consequently, the discovery of a remarkable new paracharontid in a cave system in the upper basin of the Camarones River, in the La Guajira Department of northeastern Colombia (figs. 1–3), prompted the reinvestigation of Paracharontidae presented herein.

The new troglobitic whip spider, *Jorottui ipuanai*, gen. et sp. nov., is described and *P. caecus* redescribed, based on a reexamination and reinterpretation of the newly designated lectotype. The new genus and species is the second representative of Paracharontidae and the first outside Africa. It is unambiguously assigned to the family based on several characters shared with *Paracharon*, notably a projection of the anterior carapace margin, the tritosternum not projecting anteriorly, similar pedipalp spination, a reduced number of trichobothria on the tibia of leg IV, and cushionlike female gonopods. A detailed examination confirmed the absence of ocelli in both genera and the presence of three (*Paracharon*) vs. four (*Jorottui*, gen. nov.) prolateral teeth on the basal segment of the chelicera, the dorsalmost tooth bicuspid in both genera. The male gonopods of Paracharontidae are described for the first time. *Paracharonopsis cambayensis* Engel and Grimaldi, 2014, is removed from Paracharontidae and placed incertae sedis in Euamblypygi Weygoldt, 1996; amended comparative diagnoses are presented for Paracharontidae and *Paracharon*; and previous interpretations of various diagnostic characters for Paracharontidae are discussed.

MATERIAL AND METHODS

Material of the new species was collected by hand and preserved in 70% ethanol, except for one specimen preserved in 95% ethanol for DNA extraction. The coordinates of collection localities were obtained with a portable GPS device (Garmin Etrex Legend).

Material examined is deposited in the Natural History Museum of Denmark, University of Copenhagen (ZMUC), the Instituto de Ciencias Naturales, Universidad Nacional de Colombia

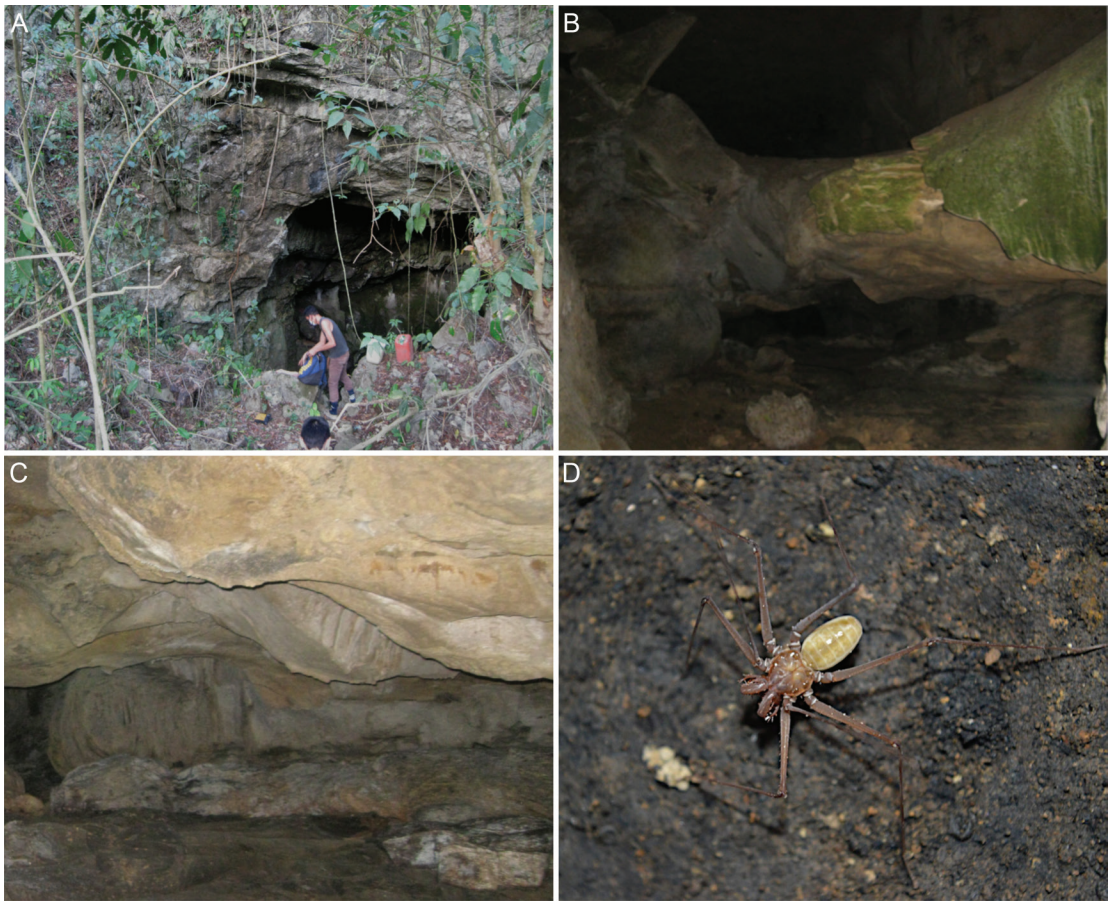

FIGURE 1. Collection locality and live habitus of *Jorottui ipuanai*, gen. et sp. nov. **A–C.** Bañaderos cave, Bañaderos, Hatonuevo, La Guajira Department, Colombia. **A.** Cave entrance. **B.** Main gallery. **C.** Microhabitat where specimens were collected. **D.** Live habitus of male from La Perrita Cave, Los Chorros, Fonseca, La Guajira Department, Colombia.

(ICN), Bogotá, and the American Museum of Natural History (AMNH), New York, with one sample in the Ambrose Monell Cryocollection (AMCC) at the AMNH.

Morphological terminology and measurements follow Quintero (1981), except for pedipalps and legs, which follow Harvey and West (1998), and male gonopods, which follow Giupponi and Kury (2013). Measurements (mm) for pedipalp segments were taken from the basal margin to the distal margin of the condyles.

Pedipalp spines are spiniform cuticular projections distinguished from setiferous tubercles by the absence of an apical seta. Primary homology assessment of the spines was determined based on position and relative size, partly following the interpretation of Garwood et al. (2017) for *P. caecus*, the comparison with which facilitated homology assessment in *Jorottui*, gen. nov. Spines shared by these taxa are referred to as "primary spines," with additional spines present in *Jorottui* referred to as "accessory spines." Comparisons with other amblypygid families and genera may facilitate homology assessment of these accessory spines. Spine nomenclature fol-

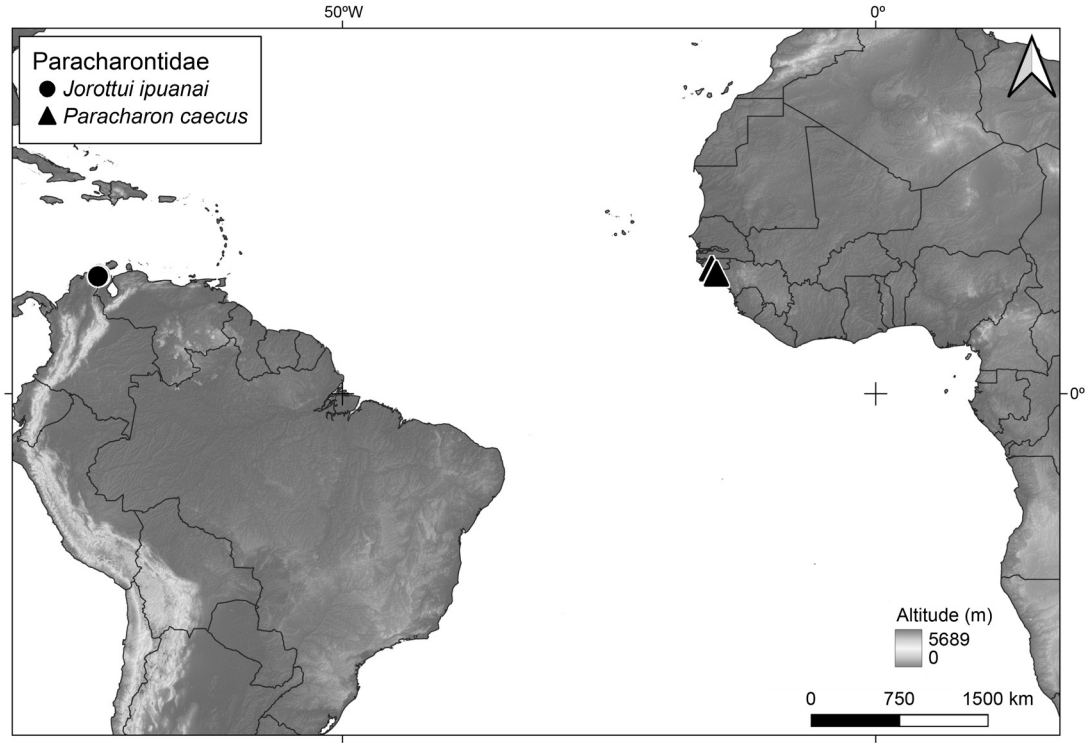

FIGURE 2. Global distribution of the family Paracharontidae Weygoldt, 1996, plotting records of *Jorottui ipuanai*, gen. et sp. nov., and *Paracharon caecus* Hansen, 1921.

lows Weygoldt (2002), using Arabic numerals for dorsal spines and Roman numerals for ventral spines. Spines are annotated from proximal to distal on the femur and from distal to proximal on the other segments.

As the pedipalps of Paracharontidae are oriented perpendicular to the body axis (i.e., vertically oriented), Weygoldt's (1996) nomenclature for the dorsal and ventral surfaces of the pedipalps of other Amblypygi taxa is, respectively, applied to the prolateral and retrolateral surfaces of the pedipalps of Paracharontidae.

Chelicerae and female gonopods were dissected for scanning electron microscopy (SEM) and cleaned in distilled water with neutral detergent by ultrasound for 1 minute. After cleaning, the female gonopods were washed with distilled water and dehydrated in an ethanol concentration gradient (70%, 80%, 90%, 96%, 100%) for 5–15 minutes per concentration. Structures were dehydrated using critical point drying, mounted on SEM stubs using adhesive copper tape, and sputter-coated with gold-palladium in a DENTON Desk II. Stubs were photographed in a Hitachi S-4700 scanning electron microscope at the AMNH Microscopy and Imaging Facility.

Photographs were taken with a Nikon DS-Qi2 camera, attached to a Nikon SMZ18 stereoscope. Image stacking was conducted with the software Nikon NIS-Elements. Focused images were edited with GIMP 2.10 (http://www.gimp.org/) and plates created using Inkscape 1.2.2 (http://www.inkscape.org/).

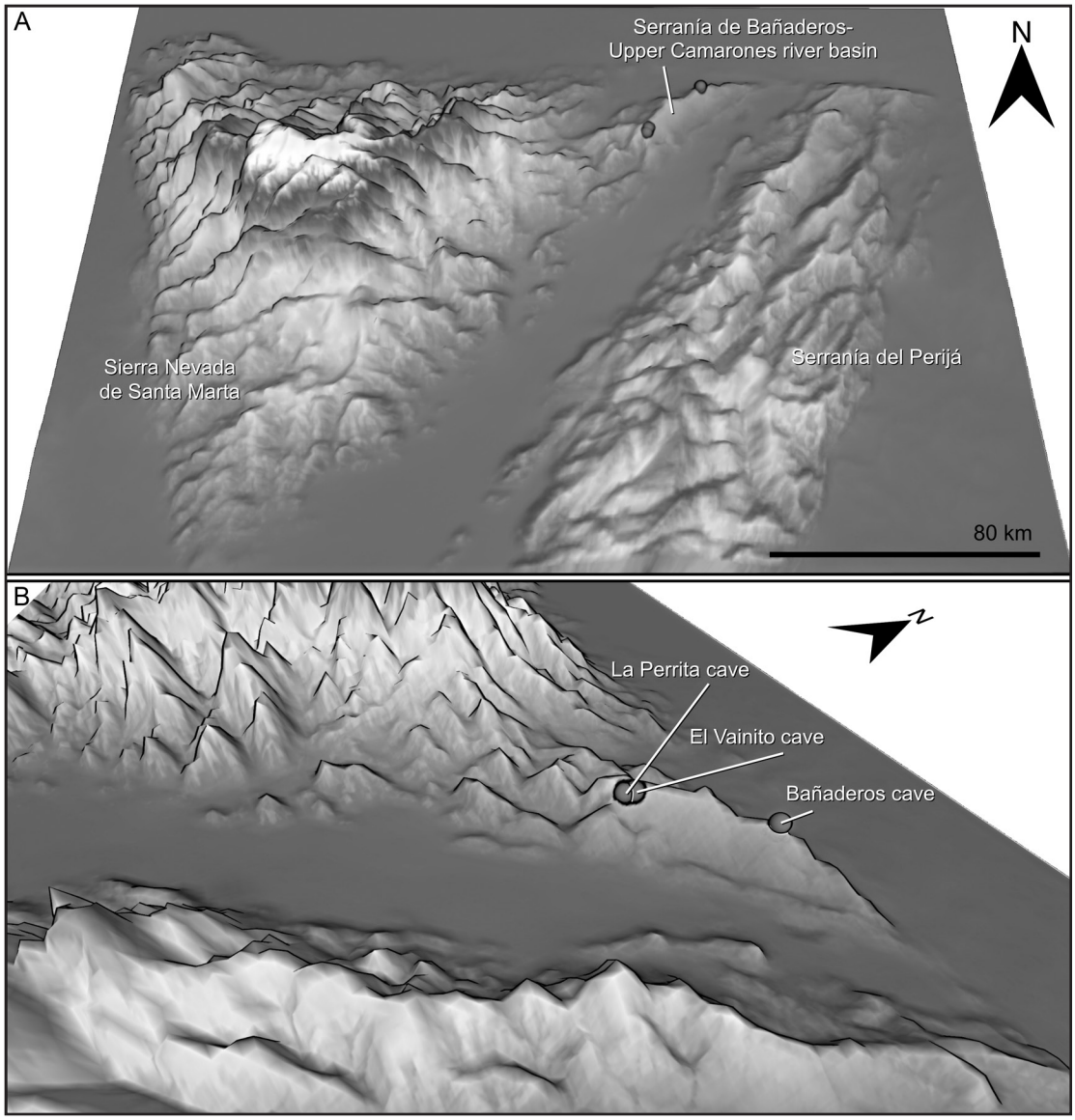

FIGURE 3. Tridimensional elevational distribution model of northeastern Colombia, including the Serranía de Bañaderos, upper basin of the Camarones River, showing the mountain ranges (**A**) and caves (**B**) in which specimens of *Jorottui ipuanai*, gen. et sp. nov., were collected.

The 2D distribution map was prepared with QGIS 3.30 (http://www.qgis.org/) using a digital elevation model (DEM), the raster Hillshade conversion (with layers on azimuths 45° and 145°) and a single band rendering (i.e., BrBg). The 3D distribution map was prepared using a DEM of northeastern Colombia and the Qgis2threejs extension of QGIS. The type localities of *P. caecus*, obtained from the WAC (2023), were retroactively georeferenced using the GeoNames Server (http://www.geonames.org/).

The following abbreviations are used in the text: male gonopods: LaM (lamina medialis), LoD (lobus dorsalis), LoL1 (lobulus lateralis primus), LoL2 (lobulus lateralis secundus), PI (processus internus); morphometrics: L (length), W (width); pedipalps: AVA (anteroventral apophysis), F (femur), P (patella), Ta (tarsus), Ti (tibia), Tr (trochanter); trichobothria: *bf* (basal frontal), *bt* (basitibial), *sc* (caudal series), *sf* (frontal series), *tc* (terminal caudal), *tf* (terminal frontal).

SYSTEMATICS

Order Amblypygi Thorell, 1883

Suborder Paleoamblypygi Weygoldt, 1996

Family Paracharontidae Weygoldt, 1996

Figures 1–20

Paracharontidae Weygoldt, 1996: 200, table 4; Harvey and West, 1998: 274; Harvey, 2002a: 473; 2002b: 364, fig. 9; 2003: 1, 2, 31, table 2; Coddington et al., 2004: 305, fig. 18.1; Dunlop and Barov, 2005: 58; Dunlop et al., 2008: 165, 172, 174, 176; Dunlop, 2010: 139; Rahmadi et al., 2010: 2; Engel and Grimaldi, 2014: 4, table 1; Dunlop and Mrugalla, 2015: 220; Réveillon and Maquart, 2015: 190; Wolff et al., 2015: 524; Beron, 2016: 95, 484, table 1; Miether and Dunlop, 2016: 113; Wolfe et al., 2016: 60; Wolff, 2016: 107; Wolff et al., 2016: 2; Garwood et al., 2017: 1, 3, 7–10, 12, 13, figs. 2, 6, 7; Wolff et al., 2017: 116; Beron, 2018: 85, 143, 469, 682, 895, 934, table 8.4; Dunlop, 2018: 14, 15, 18, fig. 1; McArthur et al., 2018: 62; Miranda et al., 2018a: 23; 2018b: 35; Miranda and Reboleira, 2019: 10; Nadein and Perkovsky, 2019: 603; Hu et al., 2020: 1; Barden and Engel, 2022: 421; Löscher et al., 2022: 2; Miranda et al., 2022: 143, 148; Réveillion et al., 2022: 10; Seiter et al., 2022: 1, 17.

Paracharonitidae: Dunlop and Barov, 2005: 58.

Diagnosis: Paracharontidae may be distinguished from all other Amblypygi by the following characters: vertically oriented pedipalps (fig. 4); anterior carapace margin conspicuously projecting (fig. 5); tritosternum not projecting anteriorly (fig. 7); tibia of leg IV with 11 trichobothria: *bt*, *bf*, sc_{1-3}, sf_{1-4}, *tc* and *tf* (fig. 19). In all other families of Amblypygi, the pedipalps are oriented horizontally or oblique to the horizontal plane; the anterior carapace margin is not conspicuously projecting; the tritosternum is projecting anteriorly; and the tibia of leg IV bears a greater and variable number of trichobothria.

Included Species: Paracharontidae currently comprises two extant, monotypic genera: *Paracharon caecus* Hansen, 1921, and *Jorottui ipuanai*, gen. et sp. nov. *Paracharonopsis cambayensis* Engel and Grimaldi, 2014, the Early Eocene amber fossil from Gujarat, India, is hereby removed from Paracharontidae for the following reasons: As noted by Haug and Haug (2021), the pedipalp orientation of *P. cambayensis* appears to be more horizontal than vertical (Engel and Grimaldi, 2014: 5, fig. 1) like Euamblypygi and unlike Paracharontidae. Furthermore, several other characters suggest that *P. cambayensis* is more closely related to Euamblypygi than to Paracharontidae. The anterior carapace margin lacks a conspicuous projection in *P. cambayensis* (Engel and Grimaldi, 2014: 5, fig. 1) unlike *Jorottui*, gen. nov., and *Paracharon* (fig. 5);

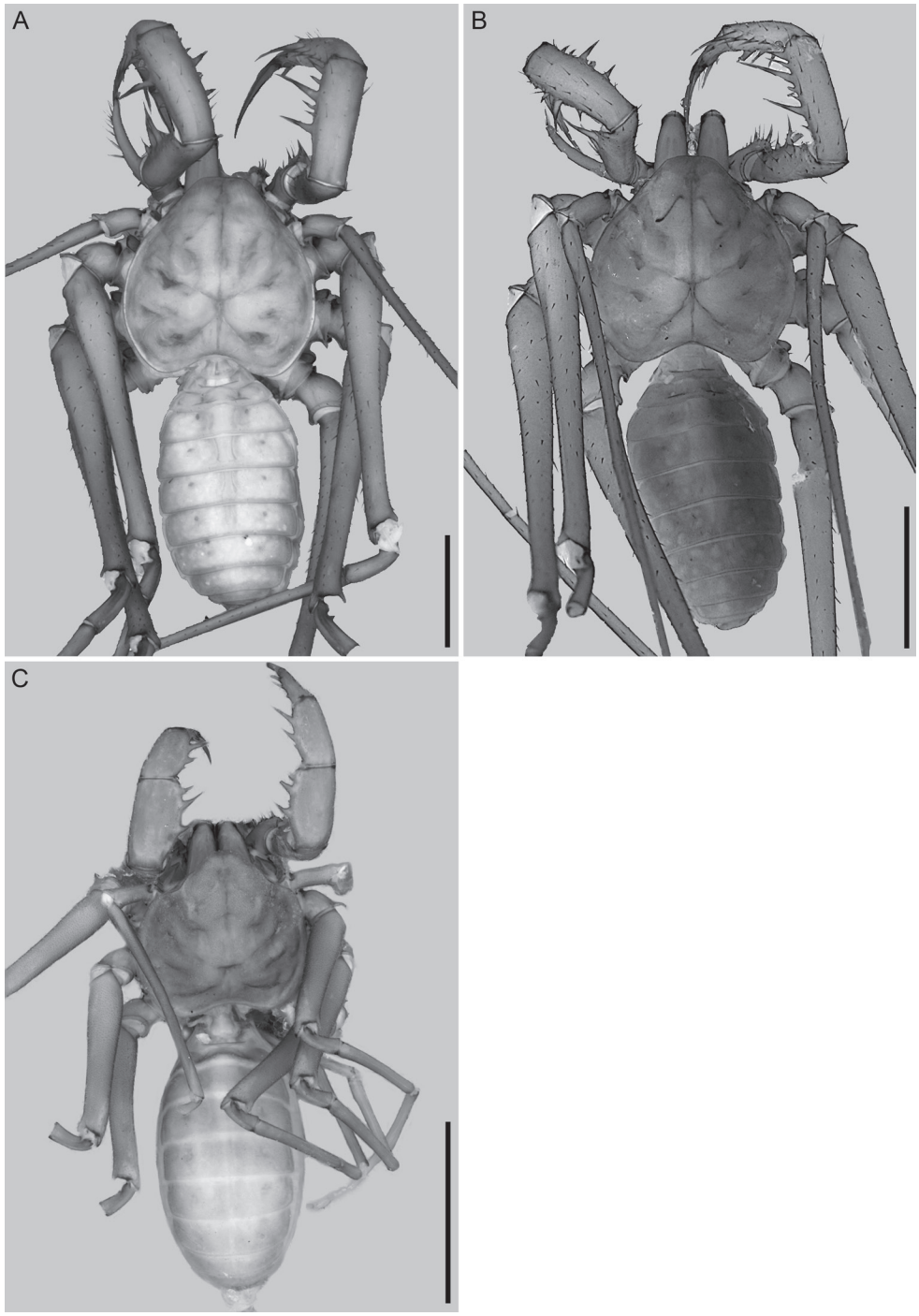

FIGURE 4. Paracharontidae Weygoldt, 1996, habitus, dorsal aspect. **A, B.** *Jorottui ipuanai*, gen. et sp. nov. **A.** Holotype ♀ (ICN-Am 180). **B.** Paratype ♂ (ICN-Am 187). **C.** *Paracharon caecus* Hansen, 1921, lectotype ♀ (ZMUC 24556). Scale bars: 3 mm.

median and lateral ocelli are present in *P. cambayensis* (Engel and Grimaldi, 2014: 7, fig. 2A) but absent in *Jorottui* and *Paracharon* (fig. 5); the pedipalp femur bears two proximal dorsal spines in *P. cambayensis* (Engel and Grimaldi, 2014: 7, fig. 2A) but one or two distal dorsal spines in *Jorottui* (fig. 14D, F) and *Paracharon* (fig. 14B), respectively; the pedipalp patella bears four primary dorsal spines, the first (distalmost) spine large and the remaining spines decreasing in size proximally in *P. cambayensis* (Engel and Grimaldi, 2014: 7, fig. 2A) whereas the patella bears three primary dorsal spines, the first (distalmost) spine small, in *Jorottui* and *Paracharon* (fig. 15B, D, F); the distitibia of leg IV possesses 13 trichobothria in *P. cambayensis* (Engel and Grimaldi, 2014: 7, fig. 2D) but 10 trichobothria in *Jorottui* and *Paracharon* (fig. 19).

Based on this assessment, *Paracharonopsis cambayensis* is hereby placed incertae sedis in Euamblypygi, pending further investigation based on phylogenetic analysis.

Distribution: Paracharontidae have been recorded in northern South America (northeastern Colombia) and West Africa (western Guinea Bissau) (fig. 2).

Remarks: Paracharontidae possess the lowest counts of trichobothria on the tibia of leg IV (11) among Amblypygi. The next lowest trichobothrial counts, of 14 trichobothria (one on the basitibia and 13 on the distitibia), occur in several species of the charinid genus *Sarax* Simon, 1892: *Sarax bengalensis* (Gravely, 1911) from India; *Sarax bispinosus* (Nair, 1943) from India and Sri Lanka; *Sarax ioanniticus* (Kristscher, 1959) from Egypt, Greece, Jordan, Israel, Italy, and Turkey; *Sarax pakistanus* (Weygoldt, 2005) from Pakistan, and *Sarax socotranus* (Weygoldt et al., 2002) from Yemen.

Paracharon Hansen, 1921

Figures 2, 4C, 5C, 6C, 7E, F, 8E, F, 10A, 11A, 13A, B, 14A, B, 15A, B, 16A, B, 17A, B, 19A; table 1

Paracharon Hansen, 1921: 10, 11; Mello-Leitão, 1931: 33, 51, 53; Werner, 1935: 470; Fage, 1939: 158, 160, fig. 4; Quintero, 1983: 50; 1986: 204, 206, fig. 28; Weygoldt, 1996: 185, 191, 194, 197, fig. 52, tables 3, 4; Harvey and West, 1998: 274; Weygoldt, 1999: 104, table 1; 2000a: 12, 14, 16, 21, 23, 86, 140, 142, fig. 141, table 1; Baptista and Giupponi, 2002: 106; Harvey, 2002a: 473; 2002b: 364, fig. 9; 2003: 31; Coddington et al., 2004: 305; Dunlop et al., 2008: 172; Rahmadi et al., 2010: 2; Engel and Grimaldi, 2014: 4, 13, table 1; Wolff et al., 2015: 524, fig. 1; Beron, 2016: 484; Wolfe et al., 2016: 60; Garwood et al., 2017: 1, 3, 6–9, 12, figs. 5–7; Beron, 2018: 85, 143, 469, 895, 934, map 7.21; Dunlop, 2018: 14, 15, 18, fig. 1; McArthur et al., 2018: 62; Miranda et al., 2018b: 51; Miranda and Reboleira, 2019: 10; Reyes-Lerma et al., 2021: 2; Miranda et al., 2022: 143.

Diagnosis: *Paracharon* shares the following characters with *Jorottui*, gen. nov.: the complete absence of ocelli (fig. 5); pedipalp femur with four primary ventral spines (fig. 14A, C, E); pedipalp patella with three primary dorsal spines and four primary ventral spines (fig. 15); pedipalp tarsus with three dorsal spines (fig. 17B, D, F) and one ventral spine (fig. 17A, C, E); and cushionlike female gonopods (fig. 20B; Weygoldt, 1999: 106, fig. 1).

Paracharon may be readily distinguished from *Jorottui* as follows: carapace anterior projection with lateral margins curved in *Paracharon* (fig. 5C) but linear in *Jorottui* (fig. 5A, B);

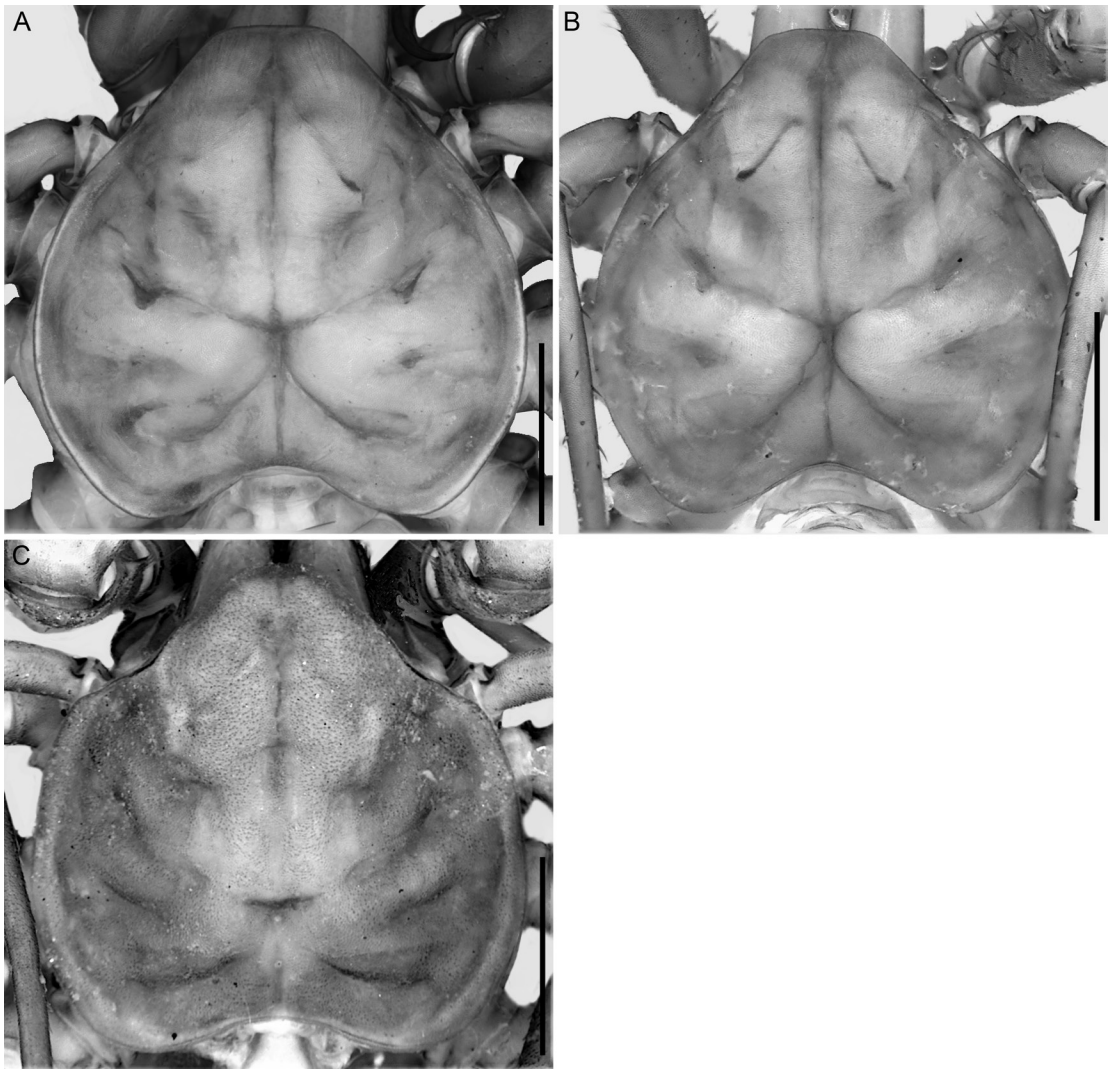

FIGURE 5. Paracharontidae Weygoldt, 1996, carapace, dorsal aspect. **A, B.** *Jorottui ipuanai*, gen. et sp. nov. **A.** Holotype ♀ (ICN-Am 180). **B.** Paratype ♂ (ICN-Am 187). **C.** *Paracharon caecus* Hansen, 1921, lectotype ♀ (ZMUC 24556). Scale bars: **A,** 0.5 mm; **B,** 0.4 mm; **C,** 0.3 mm.

prolateral margin of cheliceral basal segment with three teeth (distal tooth bicuspid) in *Paracharon* (fig. 8E) but four teeth (distal tooth bicuspid) in *Jorottui* (figs. 8A, C); ventral apophysis of pedipalp trochanter similar in length to trochanter and adorned with small setiferous tubercles in *Paracharon* (fig. 13A) but at least twice length of trochanter and adorned with large setiferous tubercles in *Jorottui* (figs. 13C, E); two dorsal spines of pedipalp trochanter short in *Paracharon* (fig. 13B) but long in *Jorottui* (fig. 13D, F); pedipalp femur with two small dorsal spines situated near distal margin in *Paracharon* (fig. 14B) but one large dorsal spine situated near distal margin in *Jorottui* (fig. 13D, F); and pedipalp tibia with three primary dorsal spines (fig. 16B) and two or three primary ventral spines (fig. 16A) in *Paracha-*

ron but four or five primary dorsal spines and four to six primary ventral spines (fig. 16C–F) in *Jorottui*.

Distribution: *Paracharon* is endemic to the West African country of Guinea Bissau, where it has been recorded at two localities, Bolama and Rio Cassine (fig. 2).

Paracharon caecus Hansen, 1921

Figures 2, 4C, 5C, 6C, 7E, F, 8E, F, 10A, 11A, 13A, B, 14A, B, 15A, B, 16A, B, 17A, B, 19A; table 1

Paracharon caecus Hansen, 1921: 11, 12, pl. 1, fig. 2A–E; 1930: pl. 14, fig. 7A; Mello-Leitão, 1931: 53; Werner, 1935: 470; Turk, 1964: 239; Cloudsley-Thompson, 1968: 156; Lawrence, 1968: 2; Mullinex, 1975: 28; Quintero, 1981: 163; 1983: 50; Delle Cave, 1986: 158; Quintero, 1986: 206, figs. 8, 28; Weygoldt, 1994: 242; 1996: 188, 191, 193–198, figs. 1, 12, 21, 34, 39, table 2; 1999: 104, fig. 1; 2000a: 14, 17, 23, 50, 86, 135, 139, figs. 14, 40–42, 103, 185; 2000b: 340, 346, fig. 2; Harvey, 2002b: 364; 2003: 31; Shultz, 2007: 249; Dunlop et al., 2008: 165, 166, 167, 172, 174, fig. 7B; Fahrein et al., 2009: 456; Penney, 2009: 72; Santer and Hebets, 2011: 3; Engel and Grimaldi, 2014: 1, 2, 13; Réveillon and Maquart, 2015: 190, 196; Beron, 2016: 484; Giupponi and Miranda, 2016: 7; Maquart and Réveillon, 2016: 27, 33; Garwood et al., 2017: 1, 3, 4, 7, 10, figs. 1C, D, 2A–F; Beron, 2018: 95, 469, 682, table 8.4; McArthur et al., 2018: 62; Miranda et al., 2018a: 24; 2018b: 35, figs. 14, 15A; Miranda and Reboleira, 2019: 9; Nadein and Perkovsky, 2019: 603; Deharveng and Bedos, 2019: 125; Haug and Haug, 2021: 406–409, table 1; Schmidt et al., 2022: 164; Miranda et al., 2022: 161.

Paracharon coecus: Fage, 1939: 153, 160; 1954: 182.

Pracharon caecus: Weygoldt, 1999: 106, fig. 1.

Type Material: The original series comprised 17 syntypes with the following data: **GUINEA BISSAU:** Bolama [11°34.629′N 15°29.237′W], vi–xii.1899, 1 ex. [sex indet.]; Rio Cassine [11°07.687′N 15°01.317′W], i–ii.1900, L. Fea, 1 ex.; same data, except 'iv.1900,' 15 ex. (ZMUC 24556). Only 2 ♀♀ (ZMUC 24556), hereby designated lectotype and paralectotype of *P. caecus*, could be located and examined for the present investigation; all other specimens are presumed lost. The specimen selected as lectotype is in better condition than the specimen selected as paralectotype.

Diagnosis: As for genus.

Description: Based on adult female lectotype (fig. 4C). Measurements (mm) in table 1.

Coloration: Body and appendages orange-brown, carapace darker (fig. 4C).

Carapace: Shape cordate (fig. 5C), as wide as long, with bumpy area anteromedially; anterior margin rounded, markedly projecting, with lateral margins curved, width of projection half width of carapace; posterior margin with shallow median notch. Two median and four pairs of dorsosubmedian transverse sulci, all distinct; anteromedian sulcus extending from anterior margin to 0.4 of carapace length, not connected to fovea; posteromedian sulcus extending from posterior margin to fovea; in anterior-posterior axis, first and third dorsosubmedian pairs of sulci not connected to fovea, second and fourth pairs connected to fovea. Median ocular tubercle, and median and lateral ocelli absent (fig. 5C). Frontal process project-

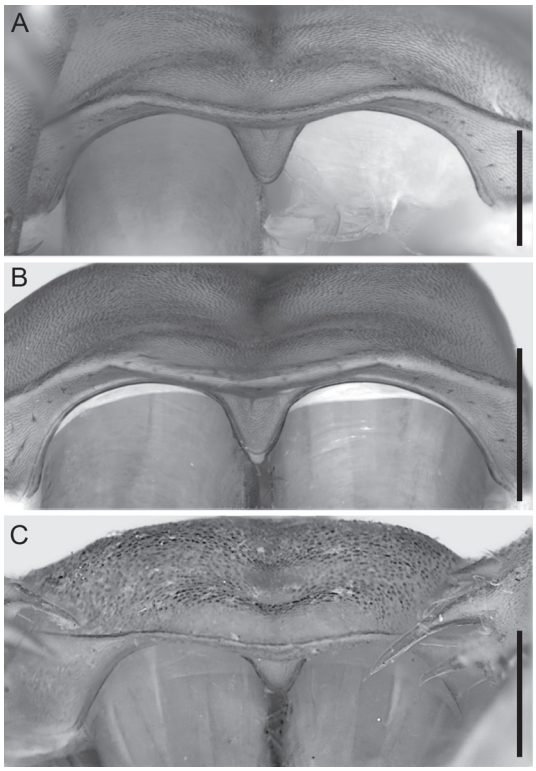

FIGURE 6. Paracharontidae Weygoldt, 1996, carapace, anterior aspect. **A, B.** *Jorottui ipuanai*, gen. et sp. nov. **A.** Paratype ♂ (ICN-Am 187). **B.** Holotype ♀ (ICN-Am 180). **C.** *Paracharon caecus* Hansen, 1921, lectotype ♀ (ZMUC 24556). Scale bars: **A, C,** 0.1 mm; **B,** 0.2 mm.

ing and recurved, 1.5× wider than long (fig. 6C). Cuticle strongly sclerotized, pigmented, apodemes barely visible.

Sterna: Tetra segmented (fig. 7E, F). Tritosternum vestigial, not projecting, consisting of single, flat, subtriangular plate, with single anteromedian microseta, pair of lateral setae and pair of posterosubmedian macrosetae. Tetrasternum comprising single plate with rounded apex bearing two setae, and with two setae on surface of plate. Pentasternum comprising single plate, projecting slightly ventrally and terminating in rounded apex bearing two setae, and with two setae on surface of plate. Metasternum comprising single subtriangular plate, anterior margin narrow, posterior margin wider, with two ventrosubmedian setae in posterior half.

Chelicerae: Basal segment, retrolateral margin without teeth but with vestigial eminence (fig. 8F); prolateral margin with three teeth (fig. 8E), first tooth (ventralmost) ca. 1.5× longer and broader than other teeth, second tooth absent, third and fourth teeth similar in size, fourth tooth (dorsalmost) bicuspid, dorsal cusp slightly larger than ventral cusp; prolateral surface with transverse row of ca. 10 setae in basal third; proventral and retroventral margins densely covered with fringe of setae (fig. 8E, F). Movable finger (claw) with nine denticles (four apparently broken) on ventral margin; prolateral surface densely covered with fringe of setae (fig. 8E).

Pedipalps: Oriented perpendicular to body in vertical plane (figs. 10A, 11A). Trochanter with moderately elongated anteroventral apophysis (AVA), ca. 1.2× longer than trochanter, terminating in small spine (fig. 13A); prolateral margin of AVA with small dorsal setiferous tubercles and row of microsetae ventral to that (fig. 13A); two dorsal primary spines (Tr1 = Tr2; fig. 13B), small setiferous tubercle distal to Tr1, two small setiferous tubercles between Tr1 and Tr2, and three small setiferous tubercles proximal to Tr2. Femur with four ventral primary spines (FII > FI > FIII > FIV; fig. 14A) and small setiferous tubercle at base of FI; femur ca. 3.8× longer than FII, FII ca. 1.45× longer than FI, ca. 2.4× longer than FIII, and ca. 4.2× longer than FIV; two dorsal primary spines (F1 = F2; fig. 14B) and small setiferous tubercle near proximal margin of segment; femur ca. 12× longer than F1 and F2. Patella with four ventral primary spines (PII > PIII > PI > PIV; fig. 15A); patella ca. 3.2× longer than PII, PII ca. 3.7× longer than PI, ca. 3.4× longer than PIII, and ca. 10× longer than PIV; three dorsal primary spines (P2 > P3 > P1; fig. 15B), small setiferous tubercle proximal to

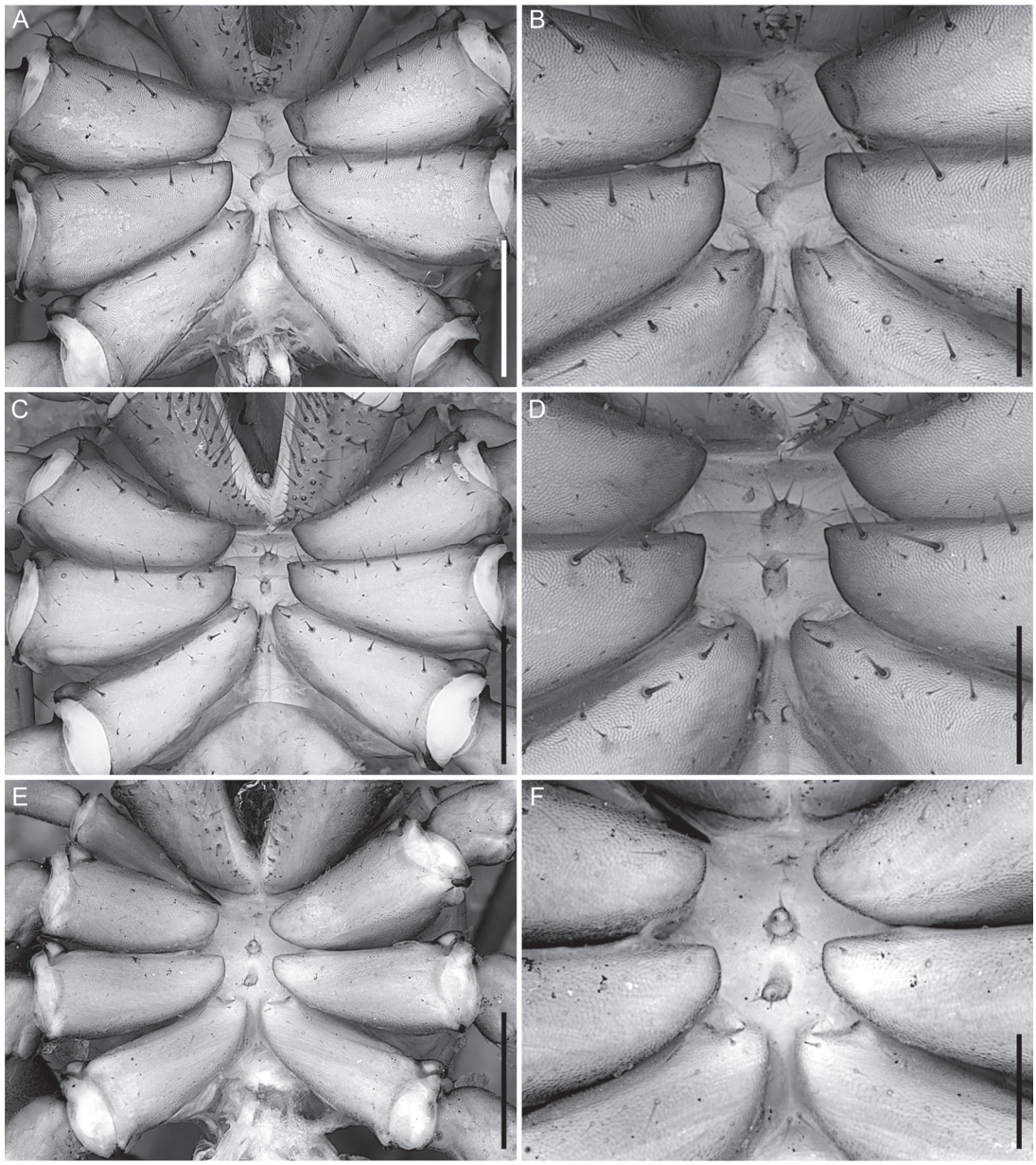

FIGURE 7. Paracharontidae Weygoldt, 1996, sternal area, ventral aspect, showing coxae (**A, C, E**) and in closeup (**B, D, F**). **A–D.** *Jorottui ipuanai*, gen. et sp. nov. **A, B.** Paratype ♂ (ICN-Am 187). **C, D.** Holotype ♀ (ICN-Am 180). **E, F.** *Paracharon caecus* Hansen, 1921, lectotype ♀ (ZMUC 24556). Scale bars: **A, E,** 0.25 mm; **B, F,** 0.1 mm; C, 0.4 mm; **D,** 0.2 mm.

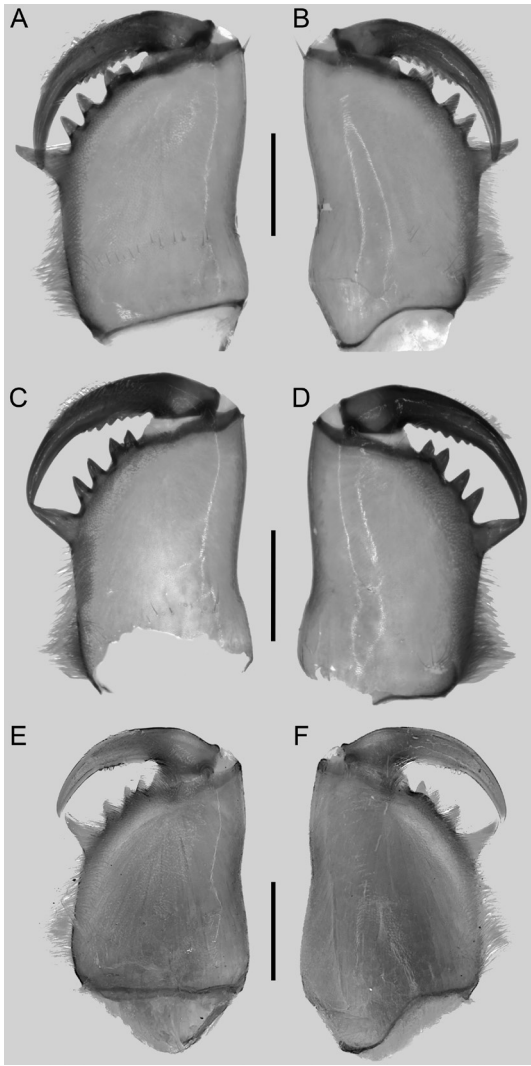

FIGURE 8. Paracharontidae Weygoldt, 1996, chelicerae, prolateral (**A, C, E**) and retrolateral (**B, D, F**) aspects. **A–D.** *Jorottui ipuanai*, gen. et sp. nov. **A, B.** Paratype ♂ (ICN-Am 187). **C, D.** Holotype ♀ (ICN-Am 180). **E, F.** *Paracharon caecus* Hansen, 1921, lectotype (ZMUC 24556). Scale bars: **A, B,** 1.5 mm; **C, D,** 1 mm; **E, F,** 0.5 mm.

P3, and small setiferous tubercle between P2 and P3; patella ca. 3.7× longer than P2, P2 ca. 1.75× longer than P1 and 1.4× longer than P3 (ratios based on sinistral pedipalp). Tibia with three ventral primary spines (TiI > TiII > TiIII; fig. 16A) (only two ventral spines on sinistral pedipalp), small setiferous tubercle proximal to TiII (only on sinistral pedipalp), and two small setiferous tubercles between TiII and TiI; tibia 2× length of TiI, TiI ca. 2.4× longer than TiII, and ca. 7× longer than TiIII (on sinistral pedipalp); three dorsal primary spines (Ti1 > Ti2 > Ti3; fig. 16B), tibia ca. 2.2× longer than Ti1, Ti1 1.9× longer than Ti2 and ca. 6.5× longer than Ti3. Tarsus with one ventral primary spine (TaI; fig. 17A); tarsus ca. 2.8× longer than TaI; three dorsal primary spines (Ta1 > Ta2 > Ta3; fig. 17B), tarsus ca. 2× length of Ta1, Ta1 ca. 1.5× longer than Ta2 and ca. 3.2× longer than Ta3. Cleaning brush organ situated along distal two-thirds of tarsus (fig. 17A); ventral setal row comprising imbricate, sickle-shaped (falcate) setae; dorsal setal row comprising curved setae; granular area densely covered with rectangular squamiform structures, each with several lipped, major glands; clavate setae, situated near cleaning organ, long and lanceolate. Claw 1.1× longer than tarsus (fig. 17A, B), curved, terminating in acute apex (fig. 17A).

Legs: Legs II–IV femora each with rounded process projecting distally. Leg I tibia and tarsus lost but, according to Weygoldt (1996), comprising 16 and 28 articles, respectively. Leg IV basitibia comprising two articles, distal third of second article with *bt* trichobothrium (fig. 19A); distitibia with 10 trichobothria: single proximal *bf* trichobothrium near articulation with basitibia, three trichobothria in *sc* series, four trichobothria in *sf* series, and single *tc* and *tf* trichobothria, all situated distally, near articulation with tarsus.

Opisthosoma: Barely translucent (contents not visible), ca. 1.8× longer than wide (fig. 4C); each tergite with pair of dorsosubmedian depressions (internal apodemes) in anterior half.

Male Genitalia: Male unknown.

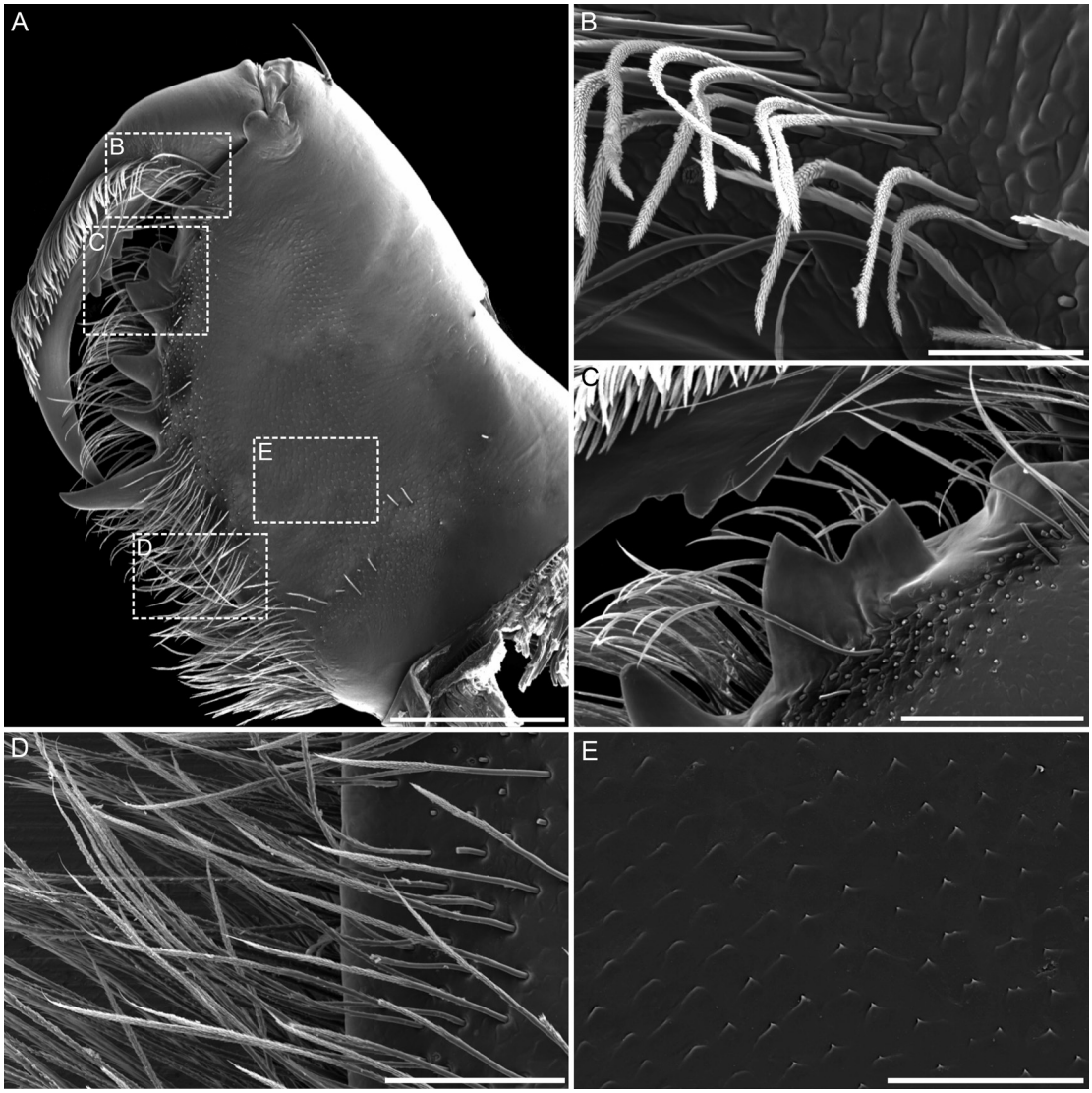

FIGURE 9. *Jorottui ipuanai*, gen. et sp. nov., paratype ♂ (ICN-Am 185), scanning electron micrographs of dextral chelicera. **A.** Prolateral aspect. **B.** Movable finger, base illustrating setae. **C.** Movable finger, serrula and basal segment, dorsal bicuspid tooth. **D.** Basal segment, ventral region, illustrating setae. **E.** Surface with minute spicules, probably stridulatory. Scale bars: **A,** 500 μm; **B,** 50 μm; **C,** 200 μm; **D, E,** 100 μm.

Female Genitalia: Based on Weygoldt (1999: 106, fig. 1), gonopods oval, globose, and cushionlike, not situated near posterior margin of genital operculum; each with soft projections, forming unsclerotized, membranous flaps, covering atrial opening; lateral flap as wide as median flap, with rounded posterior terminus and without projections on anterolateral surface; atrial opening barely visible in dorsal aspect.

Variation: Total length, 8.1 and 7.7 mm (table 1). The lectotype possesses two primary ventral spines on the sinistral pedipalp tibia and three on the dextral pedipalp tibia.

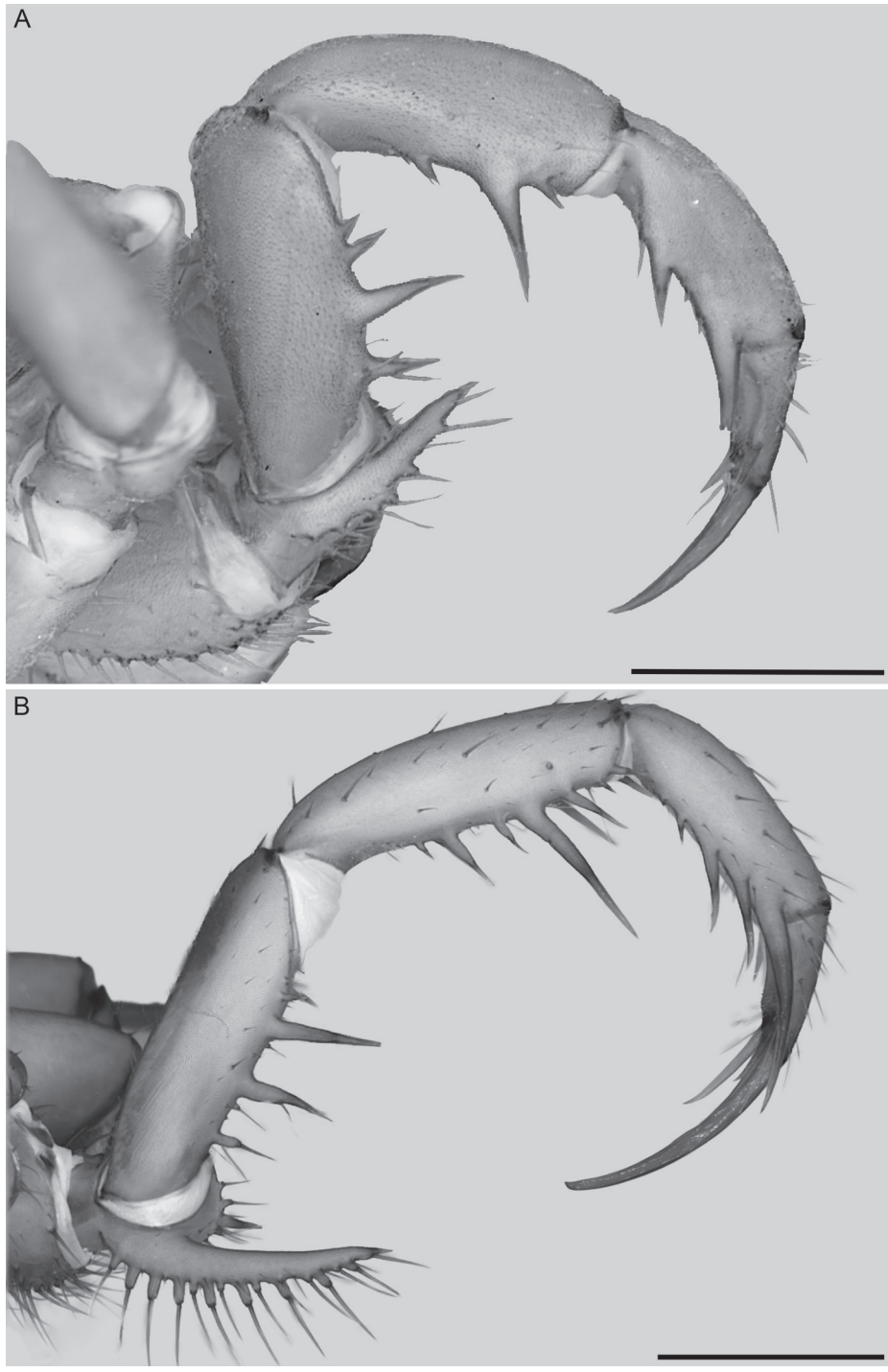

FIGURE 10. Paracharontidae Weygoldt, 1996, sinistral pedipalp (mirrored), ventral aspect. **A.** *Paracharon caecus* Hansen, 1921, lectotype ♀ (ZMUC 24556). **B.** *Jorottui ipuanai*, gen. et sp. nov., holotype ♀ (ICN-Am 180). Scale bars: **A,** 1 mm; **B,** 2 mm.

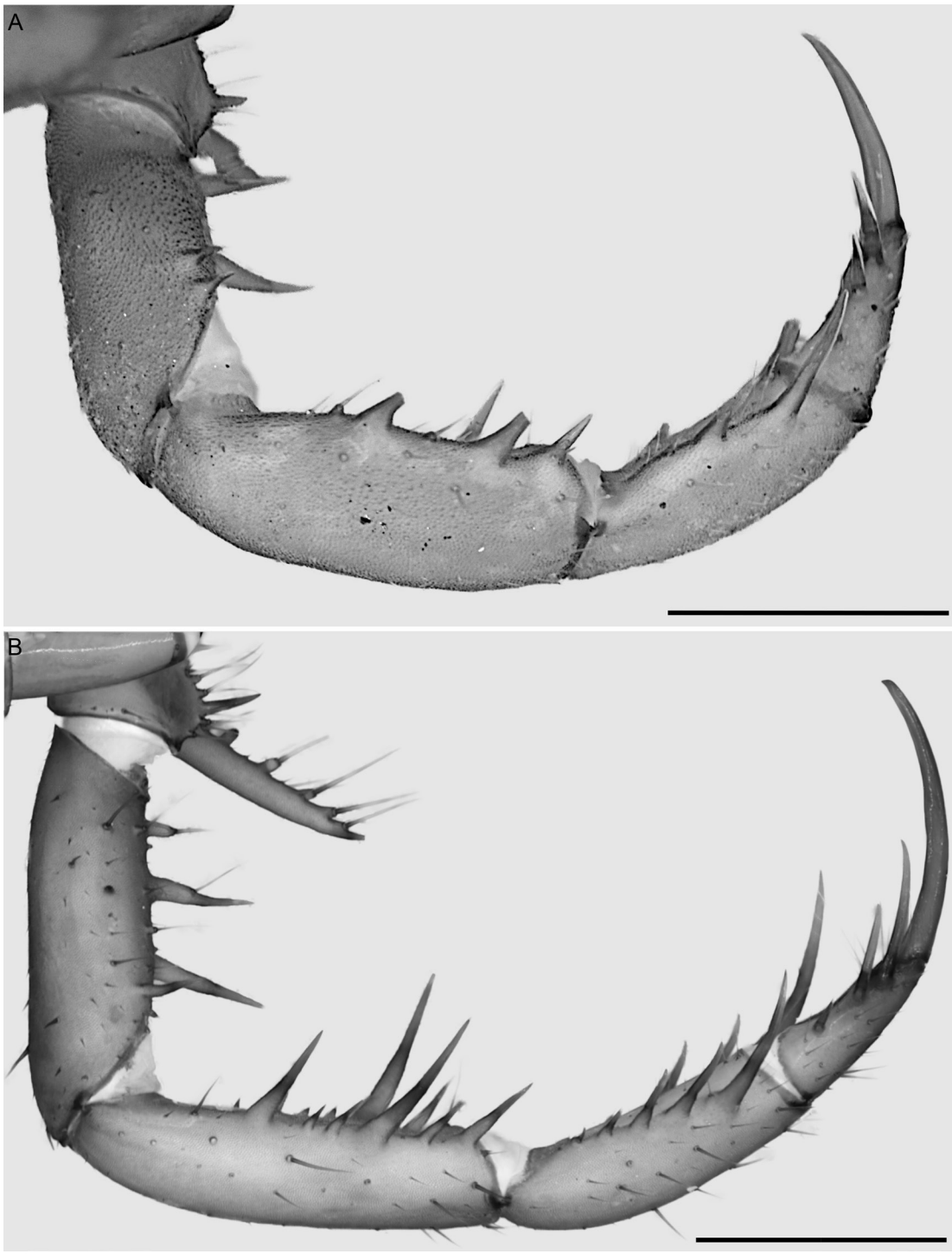

FIGURE 11. Paracharontidae Weygoldt, 1996, sinistral pedipalp (mirrored), dorsal aspect. **A.** *Paracharon caecus* Hansen, 1921, lectotype ♀ (ZMUC 24556). **B.** *Jorottui ipuanai*, gen. et sp. nov., holotype ♀ (ICN-Am 180). Scale bars: **A,** 1 mm; **B,** 2 mm.

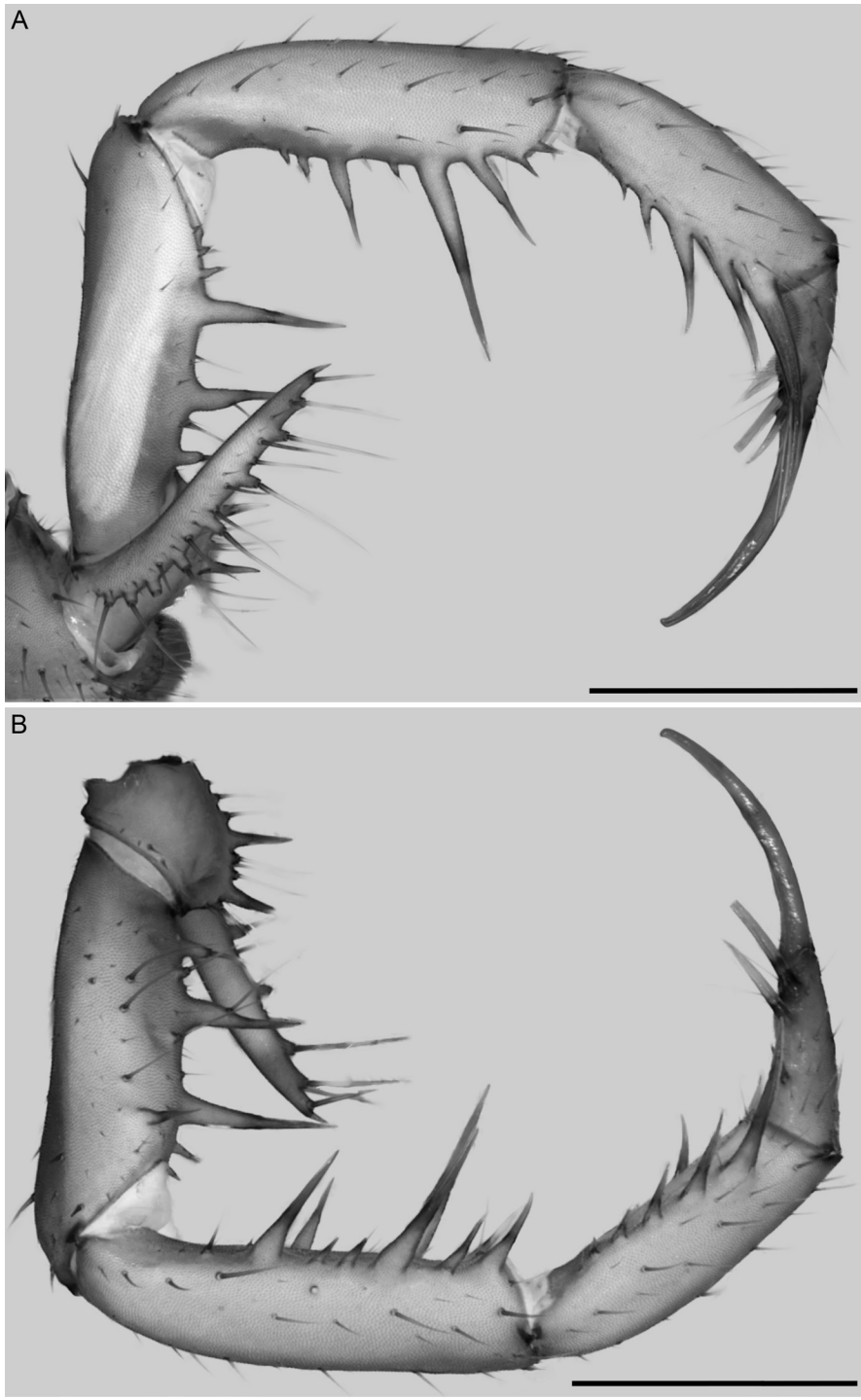

FIGURE 12. *Jorottui ipuanai*, gen. et sp. nov., paratype ♂ (ICN-Am 187), sinistral pedipalp (mirrored). **A.** Ventral aspect. **B.** Dorsal aspect. Scale bars: 1.5 mm.

Distribution: *Paracharon caecus* is known from only two localities, Bolama and Rio Cassine, in Guinea Bissau (fig. 2).

Natural History: According to Hansen (1921), the type specimens of *P. caecus* were collected inside termitaria, except for a single specimen with no information on the label. No new specimens have been collected since 1900, hence the conservation status of this species is unknown.

Jorottui, gen. nov.

Figures 1–3, 4A, B, 5A, B, 6A, B, 7A–D, 8A–D, 10B, 11B, 12, 13C–F, 14C–F, 15C–F, 16C–F, 17C–F, 18, 19B, C, 20; table 1

Diagnosis: *Jorottui*, gen. nov., shares the following characters with *Paracharon*: the complete absence of ocelli (fig. 5); pedipalp femur with four primary ventral spines (fig. 14A, C, E); pedipalp patella with three primary dorsal spines and four primary ventral spines (fig. 15); pedipalp tarsus with three dorsal spines (fig. 17B, D, F) and one ventral spine (fig. 17A, C, E); cushionlike female gonopods (fig. 20B; Weygoldt, 1999: 106, fig. 1).

Jorottui may be readily distinguished from *Paracharon* as follows: carapace anterior projection with lateral margins linear in *Jorottui* (fig. 5A, B) but curved in *Paracharon* (fig. 5C); prolateral margin of cheliceral basal segment with four teeth (distal tooth bicuspid) in *Jorottui* (fig. 8A, C) but three teeth (distal tooth bicuspid) in *Paracharon* (fig. 8E); ventral apophysis of pedipalp trochanter at least 2× length of trochanter and adorned with large setiferous tubercles in *Jorottui* (fig. 13C, E) but similar in length to trochanter and adorned with small setiferous tubercles in *Paracharon* (fig. 13A); two dorsal spines of pedipalp trochanter long in *Jorottui* (fig. 13D, F) but short in *Paracharon* (fig. 13B); pedipalp femur with one large dorsal spine situated near distal margin in *Jorottui* (fig. 14D, F) but two small dorsal spines situated near distal margin in *Paracharon* (fig. 14B); pedipalp tibia with four or five primary dorsal spines and four to six primary ventral spines (fig. 16C–F) in *Jorottui* but three primary dorsal spines (fig. 16B) and two or three primary ventral spines (fig. 16A) in *Paracharon*.

Etymology: The new genus is named after the Wayuu word "Joróttui" which means "place where perennial clarity reigns." The Wayuu people, original inhabitants of the area in which the new taxon occurs, believe Joróttui is a large cave inside the earth that represents the luminous dome of the sky. The name is a noun in apposition and is masculine in gender.

Jorottui ipuanai, sp. nov.

Figures 1–3, 4A, B, 5A, B, 6A, B, 7A–D, 8A–D, 9, 10B, 11B, 12, 13C–F, 14C–F, 15C–F, 16C–F, 17C–F, 18, 19B, C, 20; table 1

Type Material: **COLOMBIA:** *La Guajira Department*: Serranía de Bañaderos, upper basin of Camarones River: Holotype ♀ (ICN-Am 180), Hatonuevo, Bañaderos sidewalk, cave 100 m from Bañaderos Cave, 980 m, iv.2022, M. Gutierrez-Estrada. Paratypes: 1 ♀ (AMNH IZC 357368, AMCC [LP 18072]), same data as holotype; 1 ♀ (AMNH IZC 357367, AMCC [LP

TABLE 1. Meristic data (measurements in mm) for type material of *Paracharon caecus* Hansen, 1921, deposited in the Natural History Museum of Denmark, University of Copenhagen (ZMUC), and *Jorottui ipuanai*, gen. et. sp. nov., deposited in the Instituto de Ciencias Naturales, Universidad Nacional de Colombia (ICN), Bogotá and the Ambrose Monell Cryocollection (AMCC) of the American Museum of Natural History, New York. Abbreviations: **L,** length; **W,** width; **s,** sinistral; **d,** dextral.

	Paracharon caecus		*Jorottui ipuanai*					
	Lectotype ZMUC 24556 ♀	Paralectotype ZMUC 24556 ♀	Holotype ICN-Am 180 ♀	Paratype ICN-Am 181 ♀	Paratype AMNH IZC 357368 ♀	Paratype AMNH ICZ 357367 ♀	Paratype ICN-Am 190 ♂	Paratype ICN-Am 182 ♂
Total size: L	8.11	7.72	11.1	11.2	10.99	9.95	8.98	8.92
Carapace, L/W	3.32/3.05	3.15/2.93	4.84/ 5.17	5.11/4.73	5.17/ 5.22	3.97/4.46	3.70/ 4.03	3.32/ 3.32
Opisthosoma, L/W	4.79/2.61	4.57/2.67	6.26/ 3.75	6.09/3.15	5.82/ 3.92	5.98/3.26	5.28/ 3.26	5.60/ 3.05
Pedipalp: L	6.82	6.71	19.09	14.12	18.55	12.35	10.97	7.73
Trochanter	0.79	0.79	1.90	1.37	1.85	1.26	0.90	0.72
Femur	1.73	1.62	4.95	3.36	4.52	2.89	2.78	1.84
Patella	1.66	1.62	4.90	3.43	4.41	2.89	2.64	1.73
Tibia	1.19	1.19	3.59	2.60	3.26	2.13	2.02	1.37
Tarsus	0.72	0.76	1.41	1.37	1.96	1.26	1.05	0.79
Claw	0.72	0.72	2.34	1.99	2.56	1.91	1.59	1.26
Leg I: L	–	–	51.14	–	–	53.53	–	46.68
Trochanter	1.09	1.14	1.47	1.47	1.47	1.14	1.41	0.98
Femur	4.08	4.13	13.87	15.50	15.07	13.27	19.53	10.66
Patella	0.44	0.49	0.65	0.82	0.82	0.76	0.82	0.54
Tibia	–	–	19.37	–	18.99	20.73	–	19.86
Tarsus	–	–	15.78	–	–	17.63	–	14.63
Leg IV: L	11.97	12.21	32.26	–	26.87	29.00	32.53	21.49
Trochanter	1.03	1.03	2.01	1.85	1.47	1.69	1.80	1.31
Femur	3.26	3.54	10.44	9.03	7.34	8.60	10.77	6.80
Patella	0.82	0.82	1.47	1.69	1.20	1.31	1.47	0.98
Basitibia	2.61	2.56	10.23	–	9.14	9.57	10.39	6.26
Distitibia	2.45	2.35	4.73	–	4.35	4.68	4.46	3.10
Basitarsus	1.20	1.30	2.12	–	2.01	1.96	2.23	1.85
Other tarsal segments	0.60	0.61	1.25	–	1.36	1.20	1.41	1.20
Articles, tibiae I (s/d)	–	–	16/16	–/16	–/16	16/16	16/–	–/16
Articles, tarsi I (s/d)	–	–	21?/31	–/42	–	33/33	–/14?	–/33

TABLE 1 *continued*

	Jorottui ipuanai							
	Paratype ICN-Am 183	Paratype ICN-Am 184	Paratype ICN-Am 186	Paratype ICN-Am 187	Paratype ICN-Am 189	Paratype ICN-Am 185	Paratype ICN-Am 188	Paratype AMNH IZC 357366
	♂	♂	♂	♂	♂	♂	♂	♂
Total size: L	10.33	10.44	7.4	8.33	7.88	7.17	9.24	8.86
Carapace, L/W	4.35/ 4.41	4.24/ 4.35	3.05/ 3.70	3.54/ 3.54	3.64/ 3.10	3.37/3.26	3.91/3.53	3.53/3.80
Opisthosoma, L/W	5.98/ 2.88	6.20/ 3.37	4.35/ 2.18	4.79/ 2.50	4.24/ 2.61	3.80/2.61	5.33/2.66	5.33/3.10
Pedipalp: L	10.72	10.51	8.27	9.30	8.27	8.12	9.75	9.53
Trochanter	1.01	1.05	0.87	0.82	0.82	0.79	1.05	0.97
Femur	2.64	2.64	2.02	2.34	2.01	1.73	2.38	2.31
Patella	2.67	2.56	1.99	2.28	1.90	1.99	2.27	2.20
Tibia	1.95	1.84	1.48	1.69	1.47	1.44	1.70	1.73
Tarsus	1.01	0.90	0.79	0.98	0.92	0.94	1.01	1.01
Claw	1.44	1.52	1.12	1.20	1.14	1.23	1.34	1.30
Leg I: L	64.41	72.19	–	56.85	47.06	–	–	–
Trochanter	1.31	1.74	1.09	1.09	0.98	0.98	0.92	1.03
Femur	17.41	17.90	12.78	12.84	11.32	9.47	12.73	11.97
Patella	0.92	0.92	0.65	0.82	0.54	0.65	0.76	0.65
Tibia	24.15	28.29	–	21.38	18.28	–	–	26.11
Tarsus	20.62	23.34	–	20.73	15.94	–	–	–
Leg IV: L	32.91	27.31	22.25	25.62	22.09	–	23.99	23.45
Trochanter	1.69	1.36	1.20	1.36	1.14	1.20	1.36	1.36
Femur	10.12	7.94	6.75	7.78	6.80	6.26	7.45	7.18
Patella	1.36	1.20	0.87	1.03	1.09	0.98	1.20	1.14
Basitibia	11.32	9.52	7.72	8.70	7.34	–	7.83	7.51
Distitibia	5.11	4.13	3.26	3.81	3.26	–	3.54	3.48
Basitarsus	2.07	1.96	1.52	1.74	1.52	–	1.63	1.69
Other tarsal segments	1.25	1.20	0.92	1.20	0.92	–	0.98	1.09
Articles, tibiae I (s/d)	22/22	16/–	–/10?	–/16	–/16	–	–	16/–
Articles, tarsi I (s/d)	37/44	–/33	–	–/33	–/33	–	–	–

19086]), same locality as the holotype, 28.x.2022, M. Gutirrez-Estrada; 1 ♀ [poorly sclerotized] (ICN-Am 181), Hatonuevo, Bañaderos Sidewalk, Bañaderos Cave, 11°07′51.5″N 72°47′23.9″W, 1005 m, x.2015, M. Gutierrez-Estrada; 8 ♂♂ (ICN-Am 182–188, AMNH IZC 357366), Fonseca, Los Chorros sidewalk, La Perrita Cave, 11°00′22″N 72°55′00.4″W, 968 m, 11.x.2015, M. Gutierrez-Estrada; 1 ♂ (ICN-Am 189), Fonseca, Los Chorros sidewalk, La Perrita Cave, 11°00′22″N 72°55′00.4″W, 968 m, 13.i.2017, M. Gutierrez-Estrada; 1 ♂ (ICN-Am 190), Barrancas, El Vainito Cave, 11°01′04.2″N 72°54′45.1″W, 998 m, x.2021 M. Gutierrez-Estrada.

Diagnosis: As for genus.

Etymology: This new species is named after Ramón Paz Ipuana (1937–1992), a Venezuelan Wayuu educator, researcher, linguist, poet and writer, who devoted his life to studying Wayuu culture and promoting the rights and traditions of Wayuu people.

Description: Based on adult male and female (fig. 4A, B). Measurements (mm) in table 1.

Coloration: Carapace and opisthosoma light reddish brown; chelicerae, pedipalps, and legs reddish brown; tibiae and tarsi of legs, light brown (fig. 1D).

Carapace: Shape cordate (fig. 5A, B), as wide as long, without bumpy area anteromedially; anterior margin truncate, markedly projecting, with lateral margins linear, width of projection half width of carapace; posterior margin with deep median notch. Two median and four pairs of dorsosubmedian transverse sulci, all distinct; anteromedian sulcus extending from anterior margin to 0.6 of carapace length, connected to fovea; posteromedian sulcus extending from posterior margin to fovea; in anterior-posterior axis, first and third dorsosubmedian pairs of sulci not connected to fovea, second and fourth pairs connected to fovea. Median ocular tubercle, and median and lateral ocelli absent (fig. 5A, B). Frontal process projecting and recurved, 1.4× wider than long (fig. 6A, B). Cuticle feebly sclerotized, translucent, apodemes clearly visible.

Sterna: Tetra segmented (fig. 7A–D). Tritosternum vestigial, not projecting, consisting of single, flat, suboval plate, with single anteromedian seta and two pairs of lateral microsetae. Tetrasternum comprising single plate with rounded (♂) or bifurcate (♀) apex bearing two setae (fig. 7B, D), and with two setae anteriorly and two setae posteriorly on surface of plate. Pentasternum comprising single plate, projecting slightly ventrally and terminating in rounded apex bearing two setae, with posteromedian seta. Metasternum comprising single subtriangular plate, anterior margin narrow, posterior margin wider, with two ventrosubmedian setae in posterior half.

Chelicerae: Basal segment retrolateral margin without teeth but with vestigial eminence (fig. 8B, D); prolateral margin with four teeth (fig. 8A, C), first tooth (ventralmost) ca. 1.5× longer and broader than other teeth, second, third, and fourth teeth similar in size, fourth tooth (dorsalmost) bicuspid, dorsal cusp smaller than ventral cusp (fig. 9C); prolateral surface densely covered with minute spicules, probably stridulatory (fig. 9E) and with transverse row of ca. 12 setae in basal third; proventral and retroventral margins densely covered with fringe of setae (figs. 8A–D, 9A, D). Movable finger (claw) with seven denticles on ventral margin (fig. 9C); prolateral surface densely covered with fringe of setae (figs. 8A, C, 9A, B).

Pedipalps: Oriented perpendicular to body in vertical plane (figs. 10B, 11B, 12A, B). Trochanter with extremely elongated anteroventral apophysis (AVA), ca. 2× length of trochanter, termi-

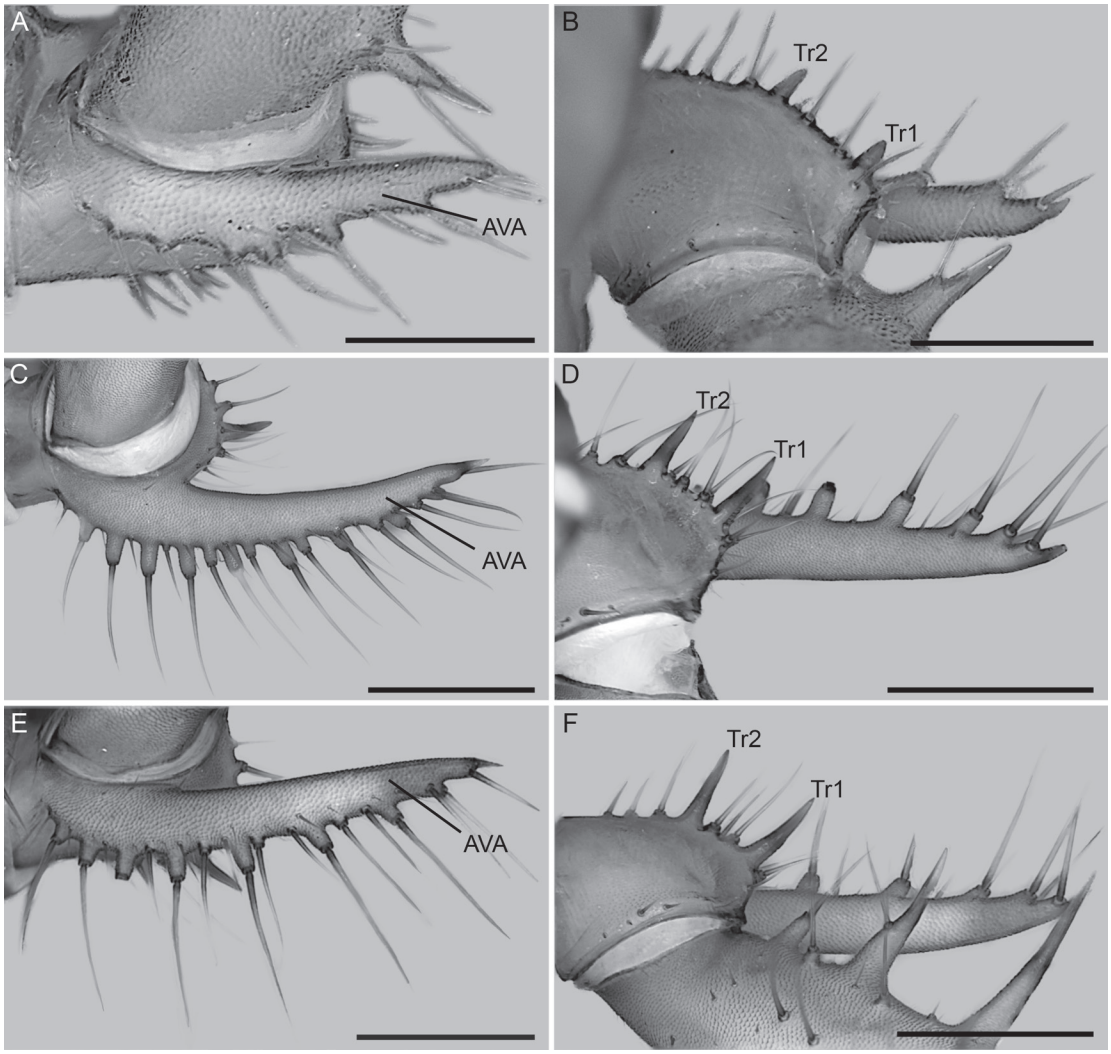

FIGURE 13. Paracharontidae Weygoldt, 1996, sinistral pedipalp trochanter (mirrored), ventral (**A, C, E**) and dorsal (**B, D, F**) aspects. **A, B.** *Paracharon caecus* Hansen, 1921, lectotype ♀ (ZMUC 24556). **C–F.** *Jorottui ipuanai*, gen. et sp. nov. **C, D.** Holotype ♀ (ICN-Am 180). **E, F.** Paratype ♂ (ICN-Am 187). Abbreviations: **AVA,** anteroventral apophysis; **Tr1,** trochanter first dorsal spine; **Tr2,** trochanter second dorsal spine. Scale bars: **A, B,** 0.4 mm; **C, E, F,** 1 mm; **D,** 1.5 mm.

nating in small spine (fig. 13C, E); prolateral margin of AVA with row of large dorsal setiferous tubercles, row of small ventral setiferous tubercles, and row of microsetae ventral to small setiferous tubercles; two dorsal primary spines (Tr1 = Tr2; fig. 13D, F), small setiferous tubercle distal to Tr1, two small setiferous tubercles between Tr1 and Tr2, and three small setiferous tubercles proximal to Tr2. Femur with four ventral primary spines (FII > FI > FIII > FIV; fig. 14C, E), large setiferous tubercle proximal to FI, and one (♂; fig. 14E) small accessory spine distal to FIV; femur ca. 3× longer than FII, FII ca. 1.3× longer than FI, ca. 4.6× (♂; fig. 14E) to 4.8× (♀; fig. 14C) longer than FIII, and ca. 8× longer than FIV; one dorsal primary spine (F1; fig. 14D, F) and two

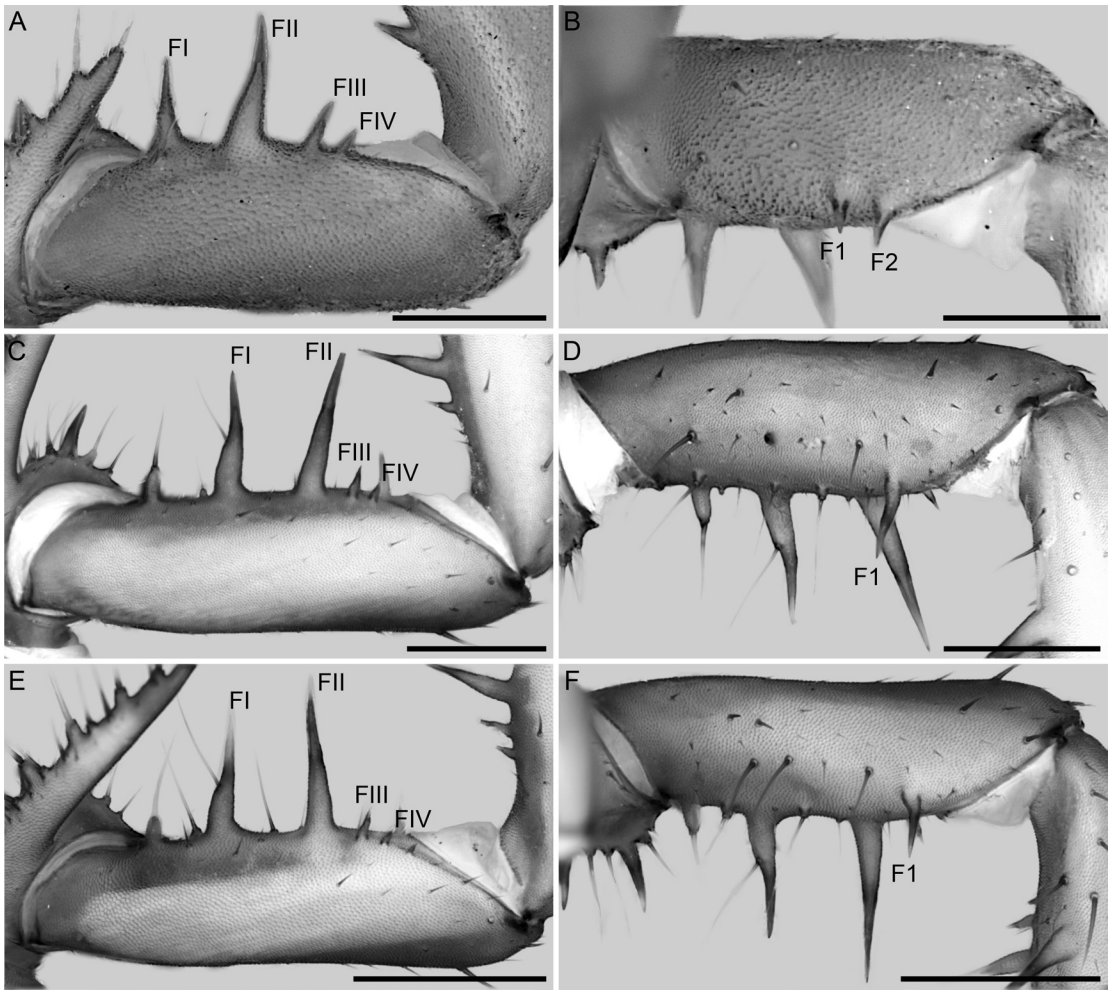

FIGURE 14. Paracharontidae Weygoldt, 1996, dextral pedipalp femur, ventral (**A, C, E**) and dorsal (**B, D, F**) aspects. **A, B.** *Paracharon caecus* Hansen, 1921, lectotype ♀ (ZMUC 24556). **C–F.** *Jorottui ipuanai*, gen. et sp. nov. **C, D.** Holotype ♀ (ICN-Am 180). **E, F.** Paratype ♂ (ICN-Am 187). Abbreviations: **F1, 2,** femur dorsal spines 1 and 2; **FI–IV,** femur ventral spines I–IV. Scale bars: **A, B,** 0.5 mm; **C–F,** 1 mm.

(♂; fig. 14D) to four (♀; fig. 14F) small, setiferous tubercles proximal to F1; femur ca. 6.3× (♀) to 7.6× (♂) longer than F1. Patella with four ventral primary spines (PII > PI > PIII > PIV; fig. 15C, E), one (♂; fig. 15E) small accessory spine proximal to PIV, one between PIII and PII, and two distal to PI; patella ca. 2.1× longer than PII, PII ca. 2× (♂; fig. 15C) to 2.4× (♀; fig. 15E) longer than PI, ca. 2.2× (♂) to 2.5× (♀) longer than PIII, and ca. 7× longer than PIV; three dorsal primary spines (P2 > P3 > P1; fig. 15D, F), small setiferous tubercle proximal to P3, two accessory spines between P3 and P2, one between P2 and P1, and one distal to P1; patella ca. 2.3× (♂; fig. 15F) to 2.5× (♀; fig. 15D) longer than P2, P2 ca. 1.9× (♂) to 1.76× (♀) longer than P1 and ca. 1.3× (♂) to 1.4× (♀) longer than P3. Tibia with five ventral primary spines (TiI > TiII > TiIII > TiIV > TiV; fig. 16C, E), tibia ca. 1.3× (♂; fig. 16E) to 1.4× (♀; fig. 16C) longer than TiI, TiI ca.

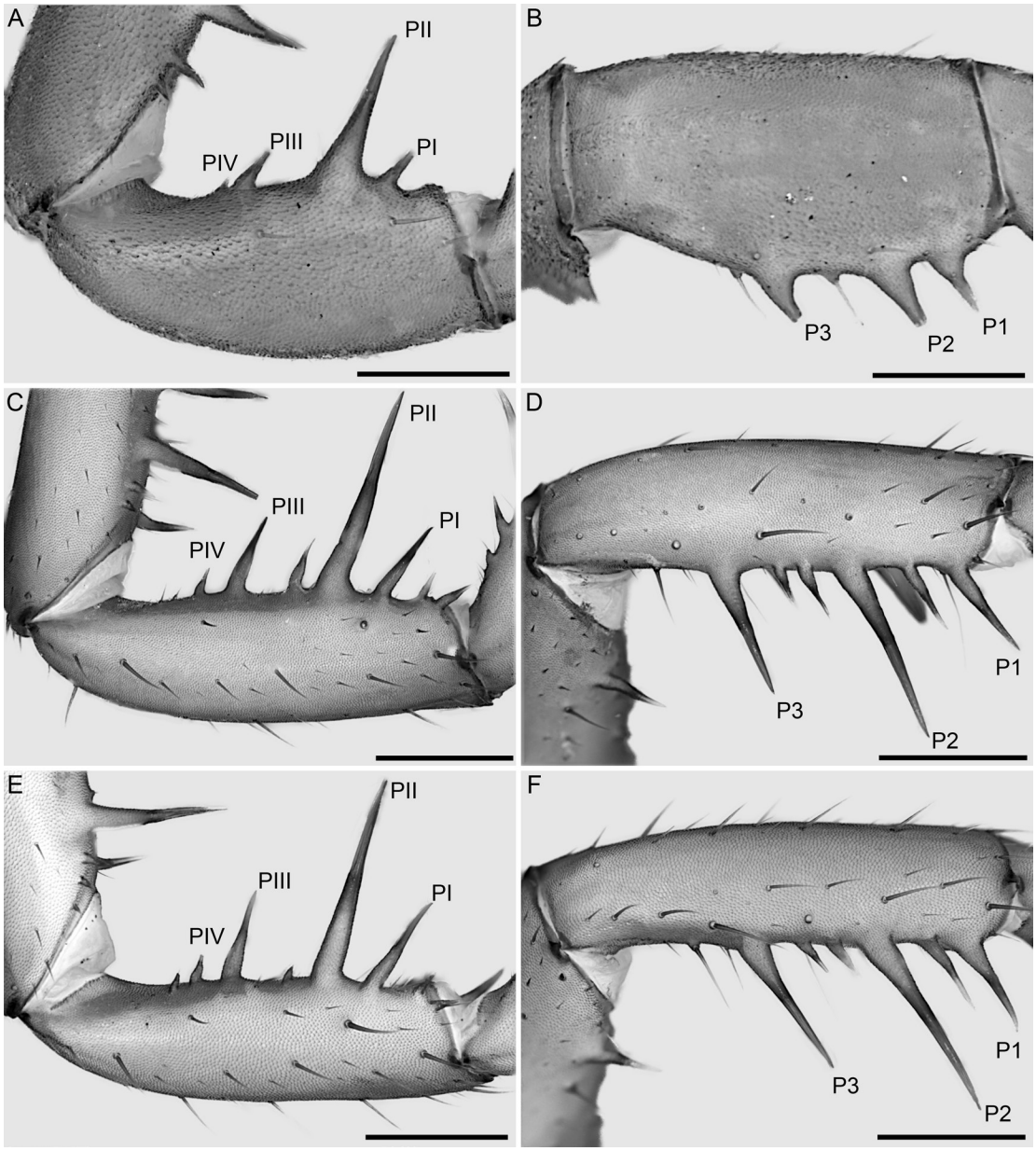

FIGURE 15. Paracharontidae Weygoldt, 1996, dextral pedipalp patella, ventral (**A, C, E**) and dorsal (**B, D, F**) aspects. **A, B.** *Paracharon caecus* Hansen, 1921, lectotype ♀ (ZMUC 24556). **C–F.** *Jorottui ipuanai*, gen. et sp. nov. **C, D.** Holotype ♀ (ICN-Am 180). **E, F.** Paratype ♂ (ICN-Am 187). Abbreviations: **P1–3,** patella dorsal spines 1–3; **PI–IV,** patella ventral spines I–IV. Scale bars: **A, B,** 0.5 mm; **C, D,** 1 mm; **E, F,** 1.5 mm.

2.1× (♂) to 2.2× (♀) longer than TiII, ca. 2.3× (♂) to 2.4× (♀) longer than TiIII, ca. 5× (♂) to 7.3× (♀) longer than TiIV, and ca. 14× (♂) to 24× (♀) longer than TiV; five dorsal primary spines (Ti1 > Ti2 > Ti3 > Ti4 > Ti5; fig. 16D, F), tibia ca. 2× length of Ti1, Ti1 ca. 1.7× longer than Ti2, ca. 2.1× (♀; fig. 16D) to 2.5× (♂; fig. 16F) longer than Ti3, ca. 3.8× longer than Ti4, and ca. 7.8×

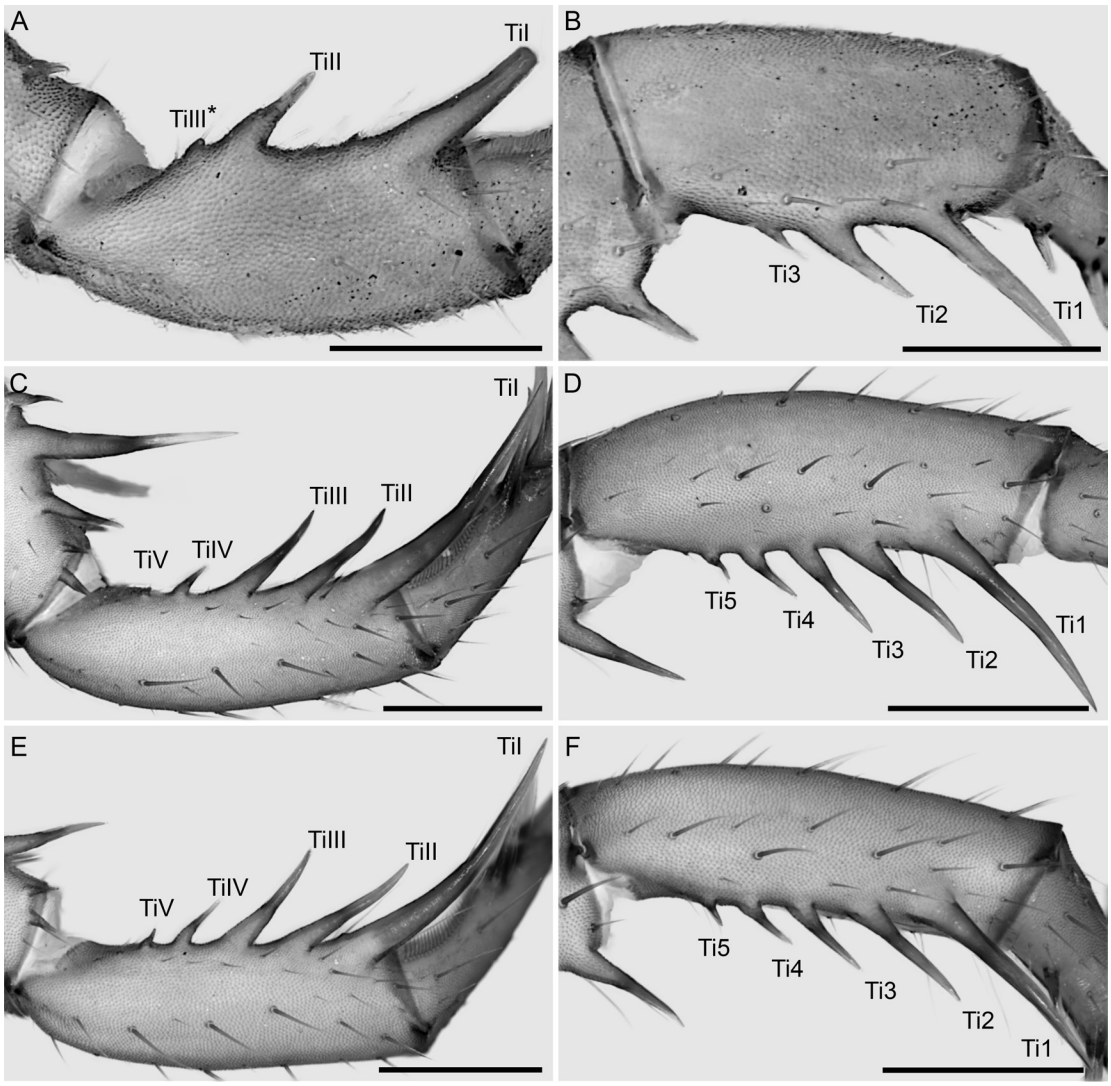

FIGURE 16. Paracharontidae Weygoldt, 1996, dextral pedipalp tibia, ventral (**A, C, E**) and dorsal (**B, D, F**) aspects. **A, B.** *Paracharon caecus* Hansen, 1921, lectotype ♀ (ZMUC 24556). **C–F.** *Jorottui ipuanai*, gen. et sp. nov. **C, D.** Holotype ♀ (ICN-Am 180). **E, F.** Paratype ♂ (ICN-Am 187). Note that spine TiIII is present only on the dextral pedipalp, whereas a setiferous tubercle is present on the sinistral pedipalp (fig. 16A). Abbreviations: **Ti1–5,** tibia dorsal spines 1–5; **TiI–IV,** tibia ventral spines I–V. Scale bars: **A, B,** 0.5 mm; **C, D,** 1 mm; **E, F,** 1.5 mm.

(♀) to 8× (♂) longer than Ti5. Tarsus with one ventral primary spine (TaI; fig. 17C, E); tarsus ca. 1.1× (♀; fig. 17C) to 1.7× (♂; fig. 17E) longer than TaI; three dorsal primary spines (Ta1 > Ta2 > Ta3; fig. 17D, F), tarsus ca. 1.1× (♂; fig. 17F) to 1.2× (♀; fig. 17D) longer than Ta1, Ta1 ca. 1.4× (♀) to 1.5× (♂) longer than Ta2, ca. 3.6× (♀) to 5.4× (♂) longer than Ta3. Cleaning brush organ (fig. 18C–F) situated along distal two-thirds of tarsus (fig. 17C, E); ventral setal row comprising imbricated, sickle-shaped (falcate) setae (fig. 18D), each with concave anterior margin; dorsal setal row comprising curved setae (fig. 18E), each covered with numerous small, lanceolate

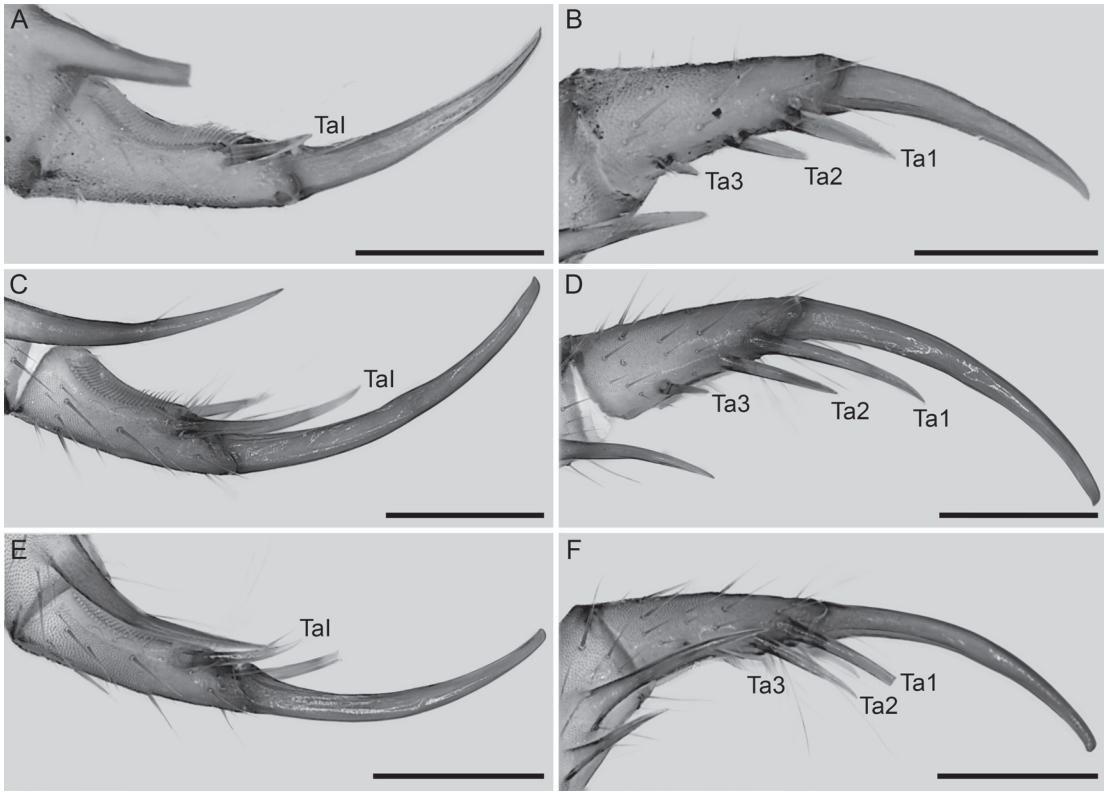

FIGURE 17. Paracharontidae Weygoldt, 1996, dextral pedipalp tarsus and claw, ventral (**A, C, E**) and dorsal (**B, D, F**) aspects. **A, B.** *Paracharon caecus* Hansen, 1921, lectotype ♀ (ZMUC 24556). **C–F.** *Jorottui ipuanai*, gen. et sp. nov. **C, D.** Holotype ♀ (ICN-Am 180). **E, F.** Paratype ♂ (ICN-Am 187). Abbreviations: **Ta1–3,** tarsus dorsal spines 1–3; **TaI,** tarsus ventral spine. Scale bars: **A, B,** 0.5 mm; **C, D,** 1 mm; **E, F,** 1.5 mm.

projections basally and dorsally; granular area densely covered with rectangular squamiform structures (fig. 18F) each with ca. 12 to >21 digitiform projections, with several lipped, major glands; clavate setae, situated near cleaning organ, long and lanceolate (fig. 18C). Claw ca. 1.3× (♂; fig. 17E) to 1.6× (♀; fig. 17C) longer than tarsus, curved, terminating in truncate apex (fig. 18A, B).

Legs: Legs II–IV femora with rounded process projecting distally. Leg I tibia comprising 16 articles; tarsus comprising 31 (holotype ♀) to 33 (paratype ♂) very elongate articles. Leg IV basitibia comprising two articles, distal third of second article with *bt* trichobothrium (fig. 19B, C); distitibia with 10 trichobothria: single proximal *bf* trichobothrium near articulation with basitibia, three trichobothria in *sc* series, four trichobothria in *sf* series, and single *tc* and *tf* trichobothria, all situated distally, near articulation with tarsus.

Opisthosoma: Translucent, ca. 1.7× longer than wide (fig. 4A, B); each tergite with pair of dorsosubmedian depressions (internal apodemes) in anterior half.

Male Genitalia: LoL1 and LoL2 similar in length and shape, both lobes becoming progressively narrower apically (fig. 20C–E); LoL1 2× width of LoL2 (fig. 20C–E); both lobes with distal half markedly curved and projecting; LoL1 and LoL2 densely covered with small digitiform projections,

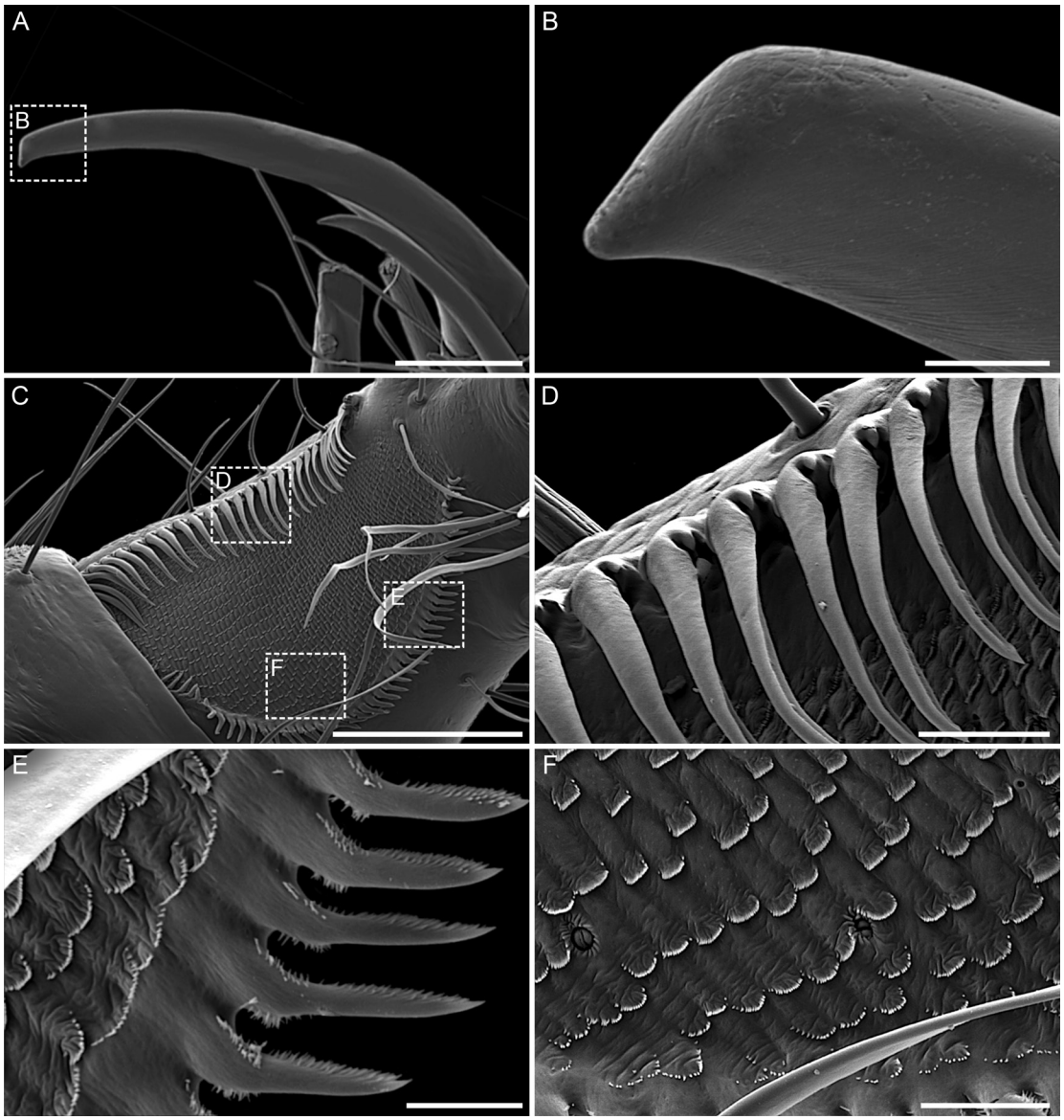

FIGURE 18. *Jorottui ipuanai*, gen. et sp. nov., paratype ♀ (ICN-Am 181), scanning electron micrographs of dextral pedipalp tarsal claw and cleaning organ. **A.** Tarsus, lateral aspect. **B.** Tarsus claw tip, illustrating truncate apex and rounded ventral projection. **C.** Cleaning organ, ventral aspect. **D.** Ventral row of cleaning organ, setae. **E.** Dorsal row of cleaning organ, setae. **F.** Granular area. Scale bars: **A,** 250 μm; **B, D,** 25 μm; **C,** 200 μm; **E,** 15 μm; **F,** 20 μm.

each with basalmost surface markedly rounded and becoming slenderer towards distal region of lobe. LoD vestigial, separated from LoL1 and LoL2 by deep groove. LaM with corrugated texture, densely covered with small digitiform projections (fig. 20E) and projecting dorsally, almost reaching ventral region of LoD. PI shorter than LaM, large, with rounded apex, visible in anterior aspect.

Female Genitalia: Gonopods oval, globose, cushionlike, situated near posterior margin of genital operculum (fig. 20B); each with soft projections, forming unsclerotized, membranous

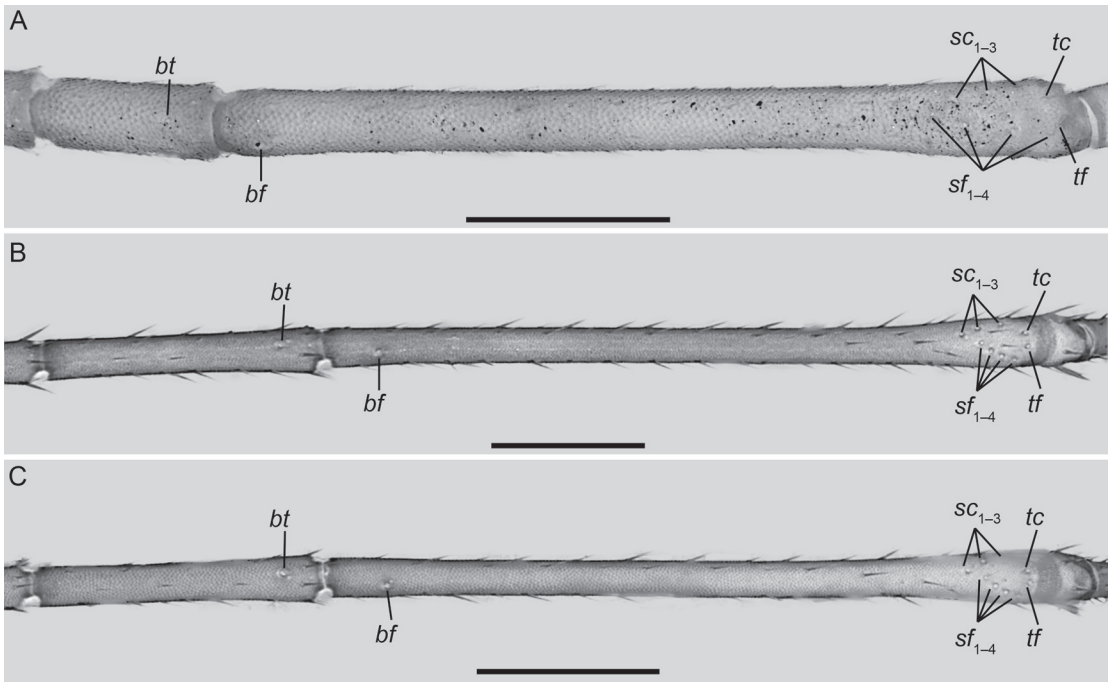

FIGURE 19. Paracharontidae Weygoldt, 1996, dextral leg IV, distal segment of basitibia and distitibia, retrolateral aspect, illustrating trichobothria. **A.** *Paracharon caecus* Hansen, 1921, lectotype ♀ (ZMUC 24556). **B, C.** *Jorottui ipuanai*, gen. et sp. nov. **B.** Holotype ♀ (ICN-Am 180). **C.** Paratype ♂ (ICN-Am 187). Abbreviations: ***bf,*** basal frontal; ***bt,*** basitibial; ***sc,*** caudal series; ***sf,*** frontal series; ***tc,*** terminal caudal; ***tf,*** terminal frontal. Scale bars: **A,** 0.5 mm; **B, C,** 1 mm.

flaps covering atrial opening; lateral flap 2× width of median flap, without projections on anterolateral surface, inner margin mostly covered by median flap, and posterior terminus rounded; inner margin of lateral flap with few visible spiniform projections anteriorly and posteriorly near areas covered by median flap; inner margin of median flap forming inconspicuous lobe medially, covering lateral flap; atrial opening barely visible in dorsal aspect.

Variation: Total length: ♂, 7.2–10.4 mm (n = 10), ♀, 10–11 mm (n = 4); Carapace L : W ratio: ♂, 0.8–1.2 (n = 10), ♀, 0.9–1.1 (n = 4); 16–22 tibial segments and 31–44 tarsal segments (table 1). Pedipalp, femur, ventral primary spines: ♂, 3–4 (n = 20 pedipalps), ♀, 4–6 (n = 8); patella, ventral accessory spines: ♂, 4–6 (n = 20 pedipalps), ♀, 4–6 (n = 7), dorsal accessory spines: ♂, 2–6 (n = 20 pedipalps), ♀, 4–5 (n = 7); tibia, ventral primary spines: ♂, 4–6 (n = 19 pedipalps), ♀, 5–6 (n = 7), dorsal primary spines, ♂, 4–5 (n = 19 pedipalps), ♀, 5 (n = 7).

Distribution: *Jorottui ipuanai*, sp. nov., is currently known from only four caves (Bañaderos Cave and an unnamed cave 100 m away from it, El Vainito Cave, and La Perrita Cave) in the Serranía de Bañaderos, a mountain range in the upper basin of the Camarones River in the La Guajira Department of northeastern Colombia (figs. 1A–C, 2, 3).

Natural History: *Jorottui ipuanai*, sp. nov., is an obligate troglobite that exhibits several troglomorphic characters such as depigmentation, thin cuticle, lack of ocelli, and elongated appendages. Several other arachnid taxa inhabit the same caves, e.g., the agoristenid harvest-

FIGURE 20. *Jorottui ipuanai*, gen. et sp. nov., scanning electron micrographs of ♂ and ♀ gonopods, dorsal aspect (**A, B**) and ♂ gonopod lobes, dorsal (**C**), ventral (**D**) and anterior (**E**) aspects. **A, C–F.** Paratype ♂ (ICN-Am 183). **B.** Paratype ♀ (ICN-Am 181). Scale bars: **A,** 500 μm; **B,** 80 μm; **C–F,** 200 μm

man, *Avima wayuunaiki* García et al., 2022, the sicariid spider, *Loxosceles guajira* Cala-Riquelme et al., 2015 (Cala-Riquelme et al., 2015; García et al., 2022), and an undescribed species of *Charinus* Simon, 1892, whip spider. The caves in which *J. ipuanai* has been collected have not been thoroughly documented or included in the national cave record of Colombia (Instituto Alexander von Humboldt, 1998). However, the area in which they are situated was recently incorporated into a protected area.

DISCUSSION

No previous study performed a thorough examination of the morphology of *Paracharon caecus*. Weygoldt (1996) scored the absence of ocelli and the presence of four prolateral teeth on the basal segment of the chelicera, with the dorsalmost tooth simple (not bicuspid), as in the fossil, *Graeophonus anglicus*. Unlike Weygoldt (1996), Garwood et al., (2017) scored *Paracharon* for the presence of lateral ocelli. Subsequently, Haug and Haug (2021) criticized some interpretations of Garwood et al. (2017), suggesting that other whip spider taxa (e.g., *Charinus desirade* Teruel and Questel, 2015) and arachnid orders (e.g., Thelyphonida) exhibit a projection of the anterior carapace margin similar to that observed in Paracharontidae, a putative synapomorphy of Paleoamblypygi, and further suggesting that the pedipalps of *Paracharonopsis* appear almost horizontally rather than vertically oriented.

These conflicting observations and interpretations can now be reevaluated in the light of evidence presented herein. For example, there is no doubt that the ocelli are completely absent in *Paracharon* (and *Jorottui*, gen. nov.; fig. 5), as reported by Weygoldt (1996, 2000a, 2000b) but contrary to Garwood et al. (2017). Also, contrary to Weygoldt (1996), *Paracharon* exhibits only three prolateral teeth, not four (unlike *Jorottui*) on the cheliceral basal segment, and the dorsalmost tooth is bicuspid (fig. 8E), as in other extant Amblypygi. However, the base of the bicuspid tooth is small and the notch between its cusps deep in *Paracharon* and *Jorottui* (fig. 8A, C, E), as in some Euamblypygi such as *Charinus milloti* Fage, 1939, and *Charinus troglobius* Baptista and Giupponi, 2022. On the other hand, a reexamination of the 3D model (stl files) of *G. anglicus* prepared by Garwood et al. (2017), corroborated their statement that this extinct species exhibits a simple prolateral dorsalmost tooth on the basal segment of the chelicera.

Another controversial character (Haug and Haug, 2021) is the projection of the anterior carapace margin, proposed as a synapomorphy for Paleoamblypygi by Weygoldt (1996) and Garwood et al. (2017). Although superficially similar in shape among some Euamblypygi, e.g., *Charinus desidare* and *Sarax seychellarum* (Kraepelin, 1898), the anterior carapace projection does not cover the cheliceral bases in these taxa, unlike in *Graeophonus*, *Paracharon*, and *Jorottui*. A similar critique applies to Thelyphonida, an order that Haug and Haug (2021) suggested exhibits a projection of the anterior carapace margin resembling that of Paleoamblypygi. Both Schizomida and Thelyphonida exhibit an anteromedian process on the prosoma (a probable homolog of the carapace ventral process of Amblypygi), which is narrow and sometimes spiniform, but not the wider projection of the ante-

rior carapace margin observed in Paleoamblypygi. Therefore, aside from their superficial similarity, the carapace shape of Paleoamblypygi is distinctly different from that of Euamblypygi, Thelyphonida, and Schizomida. Therefore, although the projection of the anterior carapace margin is probably synapomorphic for the suborder Paleoamblypygi, this needs to be tested in a phylogenetic analysis.

Furthermore, existing matrices of morphological characters for Amblypygi will need to be corrected to accommodate the observations concerning Paleoamblypygi and Paracharontidae presented herein and should be reanalyzed to reevaluate character evolution within the order and provide accurate unambiguous synapomorphies for Paleoamblypygi and Paracharontidae.

ACKNOWLEDGMENTS

The authors thank Alex González Vargas and Laura Caicedo for their assistance during the first field trip to Bañaderos cave in 2015; Nikolaj Scharff (ZMUC) for the loan of the type material of *P. caecus*; Steve Thurston (AMNH) for assistance with the plates for this contribution; and Ricardo Botero-Trujillo and Michael Seiter for constructive comments on a previous draft of the manuscript. J.A.M. was supported by grant DEB 2003382 from the U.S. National Science Foundation to L.P.

REFERENCES

Ballesteros, J.A., et al. 2022. Comprehensive species sampling and sophisticated algorithmic approaches refute the monophyly of Arachnida. Molecular Biology and Evolution 39: msac021. [https://doi.org/10.1093/molbev/msac021]

Baptista, R.L.C., and A.P.L. Giupponi. 2002. A new troglomorphic *Charinus* from Brazil (Arachnida: Amblypygi: Charinidae). Revista Ibérica de Aracnología 6: 105–110.

Barden, P., and M.S. Engel. 2022. The vision of David Grimaldi. Palaeoentomology 5: 406–429.

Beron, P. 2016. Arachnogeographical comparison between West Palearctic and Afrotropical areas. Ecologica Montenegrina 7: 464–506.

Beron, P. 2018. Zoogeography of Arachnida. Cham, Switzerland: Springer.

Cala-Riquelme, F., M.A. Gutiérrez-Estrada, and E. Flórez D. 2015. The genus *Loxosceles* Heineken and Lowe 1832 (Araneae: Sicariidae) in Colombia, with description of new cave-dwelling species. Zootaxa 4012: 396–400.

Cloudsley-Thompson, J.L. 1968. Spiders, scorpions, centipedes and mites (revised ed.). Oxford: Pergamon Press.

Coddington, J.A., G. Giribet, M.S. Harvey, L. Prendini, and D.E. Walter. 2004. Arachnida. *In* J. Cracraft and M. Donoghue (editors), Assembling the tree of life. Oxford: Oxford University Press.

Deharveng, L., and A. Bedos. 2019. Diversity of terrestrial invertebrates in subterranean habitats: 107–172. *In* O.T. Moldovan, L. Kováč, and S. Halse (editors), Cave ecology. Cham, Switzerland: Springer.

Delle Cave, L. 1986. Biospeleology of the Somaliland Amblypygi (Arachnida, Chelicerata) of the caves of the Showli Berdi and Mugdile (Bardera, Somaliland). Redia 69: 143–170.

Dunlop, J.A. 2010. Geological history and phylogeny of Chelicerata. Arthropod Structure and Development 39: 124–142.

Dunlop, J.A. 2018. Systematics of the coal measures whip spiders (Arachnida: Amblypygi). Zoologischer Anzeiger 273: 14–22.

Dunlop, J.A., and V. Barov. 2005. A new fossil whip spider (Arachnida: Amblypygi) from the Crato Formation of Brazil. Revista Ibérica de Aracnología 12: 53–62.

Dunlop, J.A., and B. Mrugalla. 2015. Redescription of the Chiapas amber whip spider *Electrophrynus mirus* (Amblypygi). Journal of Arachnology 43: 220–223.

Dunlop, J.A., G.R.S. Zhou, and S.J. Braddy. 2008. The affinities of the Carboniferous whip spider *Graeophonus anglicus* Pocock, 1911 (Arachnida: Amblypygi). Earth and Environmental Science Transactions of the Royal Society of Edinburgh 98: 165–178.

Engel, M.S., and D.A. Grimaldi. 2014. Whipspiders (Arachnida: Amblypygi) in amber from the Early Eocene and mid-Cretaceous, including maternal care. Novitates Paleoentomologicae 9: 1–17.

Fage, L. 1939. Les pédipalpes africains du genre *Charinus* à propos d'une espèce nouvelle du Fouta Djalon: *Charinus milloti*, n. sp. Bulletin de la Société Entomologique de France 44: 153–160.

Fage, L. 1954. Remarques sur la distribution géographique des pédipalpes amblypyges Africains, accompagnées de la description d'une espèce nouvelle de Madagascar: *Charinus madagascariensis*, nov. sp. Annales du Musée du Congo Belge, Sciences Zoologiques 1: 180–184.

Fahrein, K., S.E. Masta, and L. Podsiadlowski. 2009. The first complete mitochondrial genome sequences of Amblypygi (Chelicerata: Arachnida) reveal conservation of the ancestral arthropod gene order. Genome 52: 456–466.

García, A.F., A.G. Vargas, and M.G. Estrada. 2022. New records and a new cave-dwelling species of Agoristenidae (Arachnida, Opiliones) from Colombia. Zoosystematics and Evolution 98: 55–63.

Garwood, R.J., and J. Dunlop. 2014. Three-dimensional reconstruction and the phylogeny of extinct chelicerate orders. PeerJ 2: e641.

Garwood, R.J., J.A. Dunlop, B.J. Knecht, and T.A. Hegna. 2017. The phylogeny of fossil whip spiders. BMC Evolutionary Biology 17: 1–14.

Giribet, G. 2018. Current views on chelicerate phylogeny—a tribute to Peter Weygoldt. Zoologischer Anzeiger 273: 7–13.

Giupponi, A.P.L., and A.B. Kury. 2013. Two new species of *Heterophrynus* Pocock, 1894 from Colombia with distribution notes and a new synonymy (Arachnida: Amblypygi: Phrynidae). Zootaxa 3647: 329–342.

Giupponi, A.P.L., and G.S. de Miranda. 2016. Eight new species of *Charinus* Simon, 1892 (Arachnida: Amblypygi: Charinidae) endemic for the Brazilian Amazon, with notes on their conservational status. PLoS One 11: e0148277.

Hansen, H.J. 1921. The Pedipalpi, Ricinulei, and Opiliones (exc. Op. Laniatores) collected by Mr. Leonardo Fea in tropical West Africa and adjacent islands. *In* H.J. Hansen (editor), Studies on Arthropoda 1: 1–55. Copenhagen: Gyldendalske Boghandel.

Hansen, H.J. 1930. On the comparative morphology of the appendages in the Arthropoda. B. Crustacea (supplement), Insecta, Myriapoda, and Arachnida. *In* H.J. Hansen (editor), Studies on Arthropoda 3: 1–376. Copenhagen: Gyldendalske Boghandel.

Harvey, M.S. 2002a. The first Old World species of Phrynidae (Amblypygi): *Phrynus exsul* from Indonesia. Journal of Arachnology 30: 470–474.

Harvey, M.S. 2002b. The neglected cousins: What do we know about the smaller arachnid orders? Journal of Arachnology 30: 357–372.

Harvey, M.S. 2003. Catalogue of the smaller arachnid orders of the World. Amblypygi, Uropygi, Schizomida, Palpigradi, Ricinulei and Solifugae. Melbourne: CSIRO Publishing.

Harvey, M.S., and P.L.J. West. 1998. New species of *Charon* (Amblypygi, Charontidae) from northern Australia and Christmas Island. Journal of Arachnology 26: 273–284.

Haug, C., and J.T Haug. 2021. The fossil record of whip spiders: the past of Amblypygi. PalZ 95: 387–412.

Hu, X., et al. 2020. A new whip spider (Arachnida: Amblypygi) in mid-Cretaceous Kachin amber. Cretaceous Research 116: 104596.

Instituto Alexander von Humboldt. 1998. Conservación de los ecosistemas subterráneos en Colombia. Biosíntesis 10: 1–4.

Lawrence, R.F. 1968. The structure of the cleaning brush on the pedipalps of some African Amblypygi (Arachnida). Journal of Zoology, London 154: 1–8.

Legg, D.A., M.D. Sutton, and G.D. Edgecombe. 2013. Arthropod fossil data increase congruence of morphological and molecular phylogenies. Nature Communications 4: 2485.

Löscher, A., H.W. Krenn, T. Schwaha, and M. Seiter. 2022. The male reproductive system in whip spiders (Arachnida: Amblypygi). Journal of Morphology 283: 543–556.

Maquart, P.O., and F. Réveillion 2016. Les amblypyges de Guayane-Française (Arachnida: Amblypygi). Revista Ibérica de Aracnología 29: 27–33.

McArthur, I.W., G.S. de Miranda, M. Seiter, and K.J. Chapin. 2018. Global patterns of sexual dimorphism in Amblypygi. Zoologischer Anzeiger 273: 56–64.

Mello-Leitão, C. 1931. Pedipalpos do Brasil e algumas notas sobre a ordem. Arquivos do Museu Nacional, Rio de Janeiro 33: 7–72.

Miether, S.T., and J.A. Dunlop. 2016. Lateral eye evolution in the arachnids. Arachnology 17: 103–119.

Miranda, G.S. de, and A.S.P.S. Reboleira. 2019. Amblypygids of Timor-Leste: first records of the order from the country with the description of a remarkable new species of *Sarax* (Arachnida, Amblypygi, Charinidae). ZooKeys 820: 1–12.

Miranda, G.S. de, A.P.L. Giupponi, L. Prendini, and N. Scharff. 2018a. *Weygoldtia*, a new genus of Charinidae Quintero, 1986 (Arachnida, Amblypygi) with a reappraisal of the genera in the family. Zoologischer Anzeiger 273: 23–32.

Miranda, G.S. de, A.B. Kury, and A.P.L. Giupponi. 2018b. Review of *Trichodamon* Mello-Leitão 1935 and phylogenetic placement of the genus in Phrynichidae (Arachnida, Amblypygi). Zoologischer Anzeiger 273: 33–55.

Miranda, G.S. de, A.P. Giupponi, N. Scharff, and L. Prendini. 2022. Phylogeny and biogeography of the pantropical whip spider family Charinidae (Arachnida: Amblypygi). Zoological Journal of the Linnean Society 194: 136–180.

Mullinex, C.L. 1975. Revision of *Paraphrynus* Moreno (Amblypygida: Phrynidae) for North America and the Antilles. Occasional Papers of the California Academy of Sciences 116: 1–80.

Nadein, K.S., and E.E. Perkovsky. 2019. Small and common: the oldest tropical Chrysomelidae (Insecta: Coleoptera) from the lower Eocene Cambay amber of India. Alcheringa 43: 597–611.

Penney, D. 2009. Common spiders and other arachnids of the Gambia, West Africa. Manchester: Siri Scientific Press.

Petrunkevitch, A. 1955. Arachnida. *In* R.C. Moore (editor), Treatise on Invertebrate Paleontology. P, Arthropoda. 2: 42–162. Lawrence, KS: University of Kansas Press.

Prendini, L., P. Weygoldt, and W.C. Wheeler. 2005. Systematics of the *Damon variegatus* group of African whip spiders (Chelicerata: Amblypygi): evidence from behaviour, morphology and DNA. Organisms, Diversity and Evolution 5: 203–236.

Quintero, D.J. 1981. The amblypygid genus *Phrynus* in the Americas (Amblypygi, Phrynidae). Journal of Arachnology 9: 117–166.

Quintero, D.J. 1983. Revision of the amblypygid spiders of Cuba and their relationships with the Caribbean and continental American amblypygid fauna. Studies on the Fauna of Curaçao and other Caribbean Islands 65: 1–54.

Quintero, D.J. 1986. Revisión de la clasificación de amblypygidos pulvinados: creación de subordenes, una nueva familia y un nuevo género con tres nuevas especies (Arachnida: Amblypygi). *In* W.G. Eberhard, Y.D. Lubin, and B.C. Robinson (editors), Proceedings of the Ninth International Congress of Arachnology: 203–212. Panama City: Smithsonian Institution Press.

Rahmadi, C., M.S. Harvey, and J. Kojima. 2010. Whip spiders of the genus *Sarax* Simon 1892 (Amblypygi: Charinidae) from Borneo Island. Zootaxa 2612: 1–21.

Réveillion, F., and P.-O. Maquart. 2015. A new species of *Charinus* Simon, 1892 (Amblypygi, Charinidae) from termite nests in French Guiana. Zootaxa 4032: 190–196.

Réveillion, F., S. Montuire, P.-O. Maquart, C. Fétiveau, and L. Bollache. 2022. Variations in the carapace shape of whip spiders (Arachnida: Amblypygi). Journal of Morphology 283: 1003–1014.

Reyes-Lerma, A.C., et al. 2021. Insights into the karyotype evolution of Charinidae, the early-diverging clade of whip spiders (Arachnida: Amblypygi). Animals 11: 3233. [https://doi.org/10.3390/ani11113233]

Santer, R.D., and E.A. Hebets. 2011. The sensory and behavioural biology of whip spiders (Arachnida, Amblypygi). Advances in Insect Physiology 41: 1–64.

Schmidt, M., R.R. Melzer, and R.D. Bicknell. 2022. Kinematics of whip spider pedipalps: a 3D comparative morpho-functional approach. Integrative Zoology 17: 156–167.

Seiter, M., T. Schwaha, L. Prendini, S.N. Gorb, and J.O. Wolff. 2022. Cerotegument microstructure of whip spiders (Amblypygi: Euamblypygi Weygoldt, 1996) reveals characters for systematics from family to species level. Journal of Morphology 283: 428–445.

Shultz, J.W. 1990. Evolutionary morphology and phylogeny of Arachnida. Cladistics 6: 1–38.

Shultz, J.W. 2007. A phylogenetic analysis of the arachnid orders based on morphological characters. Zoological Journal of the Linnean Society 150: 221–265.

Turk, F.A. 1964. Form, size, macromutation and orthogenesis in the Arachnida: an essay. Annals of the Natal Museum 16: 236–255.

WAC (World Amblypygi Catalog). 2023. World Arachnid Catalog. Bern, Switzerland: Natural History Museum Bern. Online resource (http://wac.nmbe.ch), accessed on 18 June 2023.

Werner, F. 1935. Klasse: Arachnoidea, Spinnentiere. Pedipalpen. *In* H.G. Bronn (editor), Klassen und Ordnungen des Tierreichs 5 (IV)(8)(3): 317–490. Leipzig: Akademische Verlagsgesellschaft.

Weygoldt, P. 1994. Amblypygi. *In* C. Juberthie and V. Decu (editors), Encyclopaedia Biospeologica 1: 241–247. Moulis and Bucarest: Société de Biospéologie.

Weygoldt, P. 1996. Evolutionary morphology of whip spiders: towards a phylogenetic system (Chelicerata: Arachnida: Amblypygi). Journal of Zoological Systematics and Evolutionary Research 34: 185–202.

Weygoldt, P. 1999. Spermatophores and the evolution of female genitalia in whip spiders (Chelicerata, Amblypygi). Journal of Arachnology 27: 103–116.

Weygoldt, P. 2000a. Whip spiders (Chelicerata: Amblypygi). Their biology, morphology and systematics. Stenstrup, Denmark: Apollo Books.

Weygoldt, P. 2000b. African whip spiders. Synopsis of the Amblypygi (Chelicerata: Arachnida) reported from Africa. Memorie della Società Entomologica Italiana 78: 339–359.

Weygoldt, P. 2002. Amblypygi. *In* J. Adis (editor), Amazonian Arachnida and Myriapoda: 293–302. Moscow: Pensoft.

Wolfe, J.M., A.C. Daley, D.A. Legg, and G.D. Edgecombe. 2016. Fossil calibrations for the arthropod tree of life. Earth-Science Reviews 160: 43–110.

Wolff, J.O. 2016. Soft adhesive pads. *In* J.O. Wolff and S.N. Gorb (editors), Attachment structures and adhesive secretions in arachnids: 95–116. Cham, Switzerland: Springer.

Wolff, J.O., M. Seiter, and S.N. Gorb. 2015. Functional anatomy of the pretarsus in whip spiders (Arachnida, Amblypygi). Arthropod Structure and Development 44: 524–540.

Wolff, J.O., T. Schwaha, M. Seiter, and S.N. Gorb. 2016. Whip spiders (Amblypygi) become water-repellent by a colloidal secretion that self-assembles into hierarchical microstructures. Zoological Letters 2: 1–23.

Wolff, J.O., M. Seiter, and S.N. Gorb. 2017. The water-repellent cerotegument of whip-spiders (Arachnida: Amblypygi). Arthropod Structure and Development 46: 116–129.

All issues of *Novitates* and *Bulletin* are available on the web (https://digitallibrary.amnh.org/handle/2246/5). Order printed copies on the web from:
https://shop.amnh.org/books/scientific-publications.html

or via standard mail from:
American Museum of Natural History—Scientific Publications
Central Park West at 79th Street
New York, NY 10024

♾ This paper meets the requirements of ANSI/NISO Z39.48-1992 (permanence of paper).